

**SURFACE MODIFICATION OF ALUMINIUM -ZINC
ALLOY (AA7075) AND ITS CORROSION
CHARACTERISTICS**

ANGEL ANAK RICHARD

**MATERIALS ENGINEERING/MECHANICAL
ENGINEERING
UNIVERSITY OF MALAYA
KUALA LUMPUR**

2018

**SURFACE MODIFICATION OF ALUMINIUM -ZINC
ALLOY (AA7075) AND ITS CORROSION
CHARACTERISTICS**

ANGEL ANAK RICHARD

**SUBMITTED TO THE GRADUATE SCHOOL OF
ENGINEERING FACULTY OF MECHANICAL
ENGINEERING OF UNIVERSITY OF MALAYA, IN
PARTIAL FULFILMENT OF THE REQUIREMENTS FOR
THE DEGREE OF MASTER OF MATERIALS
ENGINEERING**

2018

UNIVERSITY OF MALAYA
ORIGINAL LITERARY WORK DECLARATION

Name of Candidate: Angel Anak Richard

Matric No: KQJ170005

Name of Degree: Master in Materials Engineering

Title of Project Paper/Research Report/Dissertation/Thesis ("this Work"):
Surface Modification of Aluminium -Zinc Alloy (Aa7075) And Its Corrosion
Characteristics

Field of Study:

I do solemnly and sincerely declare that:

- (1) I am the sole author/writer of this Work;
- (2) This Work is original;
- (3) Any use of any work in which copyright exists was done by way of fair dealing and for permitted purposes and any excerpt or extract from, or reference to or reproduction of any copyright work has been disclosed expressly and sufficiently and the title of the Work and its authorship have been acknowledged in this Work;
- (4) I do not have any actual knowledge nor do I ought reasonably to know that the making of this work constitutes an infringement of any copyright work;
- (5) I hereby assign all and every rights in the copyright to this Work to the University of Malaya ("UM"), who henceforth shall be owner of the copyright in this Work and that any reproduction or use in any form or by any means whatsoever is prohibited without the written consent of UM having been first had and obtained;
- (6) I am fully aware that if in the course of making this Work I have infringed any copyright whether intentionally or otherwise, I may be subject to legal action or any other action as may be determined by UM.

Candidate's Signature

Date:

Subscribed and solemnly declared before,

Witness's Signature

Date:

Name:

Designation

SURFACE MODIFICATION OF ALUMINIUM-ZINC ALLOY AND ITS CORROSION CHARACTERISTICS

ABSTRACT

Aluminium and its alloys are adopted in wide range of applications due to its outstanding advantageous properties such as high electrical and thermal conductivities, good corrosion resistance, highly formable, recyclable and high strength with low density. In the event of corrosive environment, pure aluminium as well as its alloys can be further enhanced through surface modification to improve its corrosive property, inhibit corrosion. In this current research, the focus is on employing novel surface modification with the formation of aluminium oxide nano-porous arrays on aluminium alloy substrate 7075 (AA7075) in order to improve the corrosion properties. Development of the oxide layer was carried out through electrochemical anodization. Subsequently, heat treatment at 450 °C for duration of 1.5 hour with the aim of improving the adhesion strength of aluminium oxide nano-porous arrays and enhance corrosion resistance. Corrosion behaviour of AA7075 is studied with justifications on material properties: adhesion strength, hardness and surface wettability. The adhesion strengths and surface hardness were evaluated by scratch test and Vickers microhardness testing machine respectively. Optical wettability was conducted to inspect surface wettability of AA7075 with utilization of video-based optical contact angle measuring system. Surface topography of the aluminium oxide nano-porous coating formed after anodization as well as heat-treated were investigated by Field Emission Scanning Electron Microscopy (FESEM) while Energy Dispersive X-ray Spectroscopy (EDS) and X-ray diffractometry (XRD) are used for examination of chemical compositions presence in the thin films developed. Heat treated sample has the best adhesion strength of aluminium oxide nano-porous layer and

the highest hardness compared to substrate and heat treated samples. Corrosion test carried out reveals that anodization ables to improve corrosion resistance of AA7075. Heat-treated AA7075 also enhanced the material properties and increase corrosion protection of with the lowest corrosion rate of 1.29×10^{-6} .

Keywords: corrosion, aluminium, surface modification

University of Malaya

SURFACE MODIFICATION OF ALUMINIUM-ZINC ALLOY AND ITS CORROSION CHARACTERISTICS

ABSTRAK

Aluminium dan aloinya diaplikasikan dalam pelbagai aplikasi disebabkan oleh sifat-sifat yang berfaedahnya seperti daya konduktif elektrik dan haba yang tinggi, rintangan kakisan yang baik, sangat boleh diperbadankan, boleh dikitar semula dan kekuatan tinggi dengan ketumpatan yang rendah. Sekiranya berlaku persekitaran yang menghakis, aluminium tulen serta aloinya boleh dipertingkatkan lagi melalui pengubahsuaian permukaan untuk memperbaiki sifat menghakisnya, menghalang kakisan. Dalam penyelidikan semasa ini, tumpuannya adalah menggunakan pengubahsuaian permukaan novel dengan pembentukan aluminium oksida nano-porous arrays pada substrat aloi aluminium 7075 (AA7075) untuk meningkatkan sifat-sifat hakisan. Pengembangan lapisan oksida dilakukan melalui anodisasi elektrokimia. Selepas itu, rawatan haba pada 450 ° C selama tempoh 1.5 jam dengan tujuan meningkatkan kekuatan lekatan aluminium oksida nano-porous arrays dan rintangan kakisan enxance. Tingkah laku kakisan AA7075 dikaji dengan justifikasi sifat bahan: kekuatan lekatan, kekerasan dan kelembapan permukaan. Kekuatan lekatan dan kekerasan permukaan dinilai dengan menggunakan mesin pengujian microhardness Vickers. Kebolehgantian optik telah dijalankan untuk memeriksa kelembapan permukaan AA7075 dengan penggunaan sistem pengukur sudut sentuh optik berasaskan video. Topografi permukaan salutan nano-poros aluminium oksida yang terbentuk selepas anodisasi serta rawatan haba disiasat oleh difraksiometer X-ray (XRD) dan Mikroskopi Pengimbasan Pelepasan Medan (FESEM) manakala Spektroskopi X-ray Spektrum (EDS) untuk pemeriksaan kehadiran komposisi kimia dalam filem nipis yang dibangunkan. Sampel anodized mempunyai kekuatan lekatan terbaik lapisan oksida aluminium oksida dan kekerasan tertinggi antara sampel abstrak

dan anil. Ia juga mempamerkan kelembapan permukaan yang lebih baik. Pendek kata, ujian kakisan yang dijalankan menunjukkan bahawa anodization mampu meningkatkan rintangan kakisan AA7075. AA7075 yang diolah juga meningkatkan sifat bahan dan meningkatkan perlindungan kakisan dengan kadar kakisan terendah sebanyak 1.29×10^{-6} .

Keywords: kakisan, aluminium, pengubahsuaian permukaan

University of Malaya

ACKNOWLEDGEMENTS

First and foremost, I would like to express my utmost gratitude to my supervisor Dr. Nazatul Liana Binti Sukiman for her guidance and valuable advises throughout the process of performing the work and preparing the reports. Her comments and suggestions helped me to improve the quality of the project and most importantly to finish the project on time. Motivations and knowledge sharing from supervisor contribute a lot in helping me to finish my work.

Secondly, I also express my deepest appreciation to Dr. Masoud Sarraf, in assisting me for experimental works and advises on the research work. I highly appreciate his dedication and helpful virtue throughout the research project. His suggestions and guidances in report writing are very much appreciated too. In addition, I also want thanks my friend, Shalini for her assistance in performing experimental lab activities. Her contributions are significant in my work as without her, this research project would not have been possible to be completed within time frame.

Not to forget to express the gratitude towards my family in supporting me and always encourage me throughout my study with love, motivations and blessings.

TABLE OF CONTENTS

surface modification of aluminium-ZINC ALLOY and its corrosion characteristics	
Abstract	iii
surface modification of aluminium-ZINC alloy and its corrosion characteristics Abstrak	v
Acknowledgements	vii
Table of Contents	viii
List of Figures	xi
List of Tables	xiii
List of Symbols and Abbreviations.....	xiv
List of Appendices	xvi
CHAPTER 1: INTRODUCTION.....	1
1.1 Overview.....	1
1.2 Problem Statement.....	3
1.3 Objective.....	4
1.4 Scope of Study.....	4
CHAPTER 2: LITERATURE REVIEW.....	6
2.1 Aluminium and Aluminium Alloys	6
2.1.1 Aluminium Alloy Designation	7
2.1.2 Temper Designation of Aluminium Alloy	11
2.1.3 Electrochemistry of Aluminium.....	12
2.1.4 Aluminium Alloy 7075 Properties	13
2.2 Overview of Corrosion	14
2.2.1 Types of Corrosion.....	15

2.2.2	Corrosion Mechanism of Aluminium Alloy	17
2.2.3	Corrosion Resistance and Hydrophobicity Mechanism	19
2.3	Surface Modification of Aluminium Alloy	21
2.3.1	Anodizing of Aluminium-metal Oxide Composite.....	21
2.3.1.1	Formation of Aluminium Nano-porous.....	24
2.3.1.2	Intermetallic Phases of Aluminium Alloys with Nano-porous ...	30
2.3.1.3	Optical Appearance of Aluminium Alloys with Nano-porous....	32
2.3.1.4	Electrochemistry of Aluminium Alloy Nano-porous.....	33
2.3.1.5	Adhesion of the Aluminium Nano-porous with Substrate	36
2.3.1.6	Wettability of Anodized Aluminium.....	37
2.3.2	Annealing of Aluminium.....	37
2.4	Corrosion Characterization Techniques	39
CHAPTER 3: METHODOLOGY		41
3.1	Preparation of Samples	42
3.1.1	Preparation of Anodized and Heat-treated Samples.....	44
3.2	Surface Characterization.....	46
3.3	Quantitative Analysis on Samples	47
3.3.1	Adhesion Strength	47
3.3.2	Microhardness	49
3.3.3	Surface Wettability	50
3.4	Corrosion Studies	51
3.4.1	Preparation of Artificial Seawater	51
3.4.2	Electrochemical Polarization.....	52
CHAPTER 4: RESULTS AND DISCUSSIONS		53
4.1	Surface Characterization.....	53

4.1.1	XRD Analysis.....	54
4.1.2	FESEM and EDX Analysis	55
4.2	Characterizations of Aluminium Oxide Nano-porous Films.....	60
4.2.1	Scratch Testing	60
4.2.2	Vickers Hardness Test.....	64
4.2.3	Electrochemical Polarization.....	65
4.2.4	Surface Wettability	68
CHAPTER 5: CONCLUSION.....		71
References		73
Appendix A		79
Appendix B		80
Appendix C		81

LIST OF FIGURES

Figure 1.1: Estimated Demand of Aluminium in Year 2016 and 2017 (Villegas, 2017)	1
Figure 1.2: Flow of Research Study Activities	5
Figure 2.1: Application of Aluminium Alloys (Burns, 2018)	7
Figure 2.2: Schematic Diagram of Several Types of Corrosion	16
Figure 2.3: Mechanism of corrosion in coated aluminium (source: Exponent Engineering and Scientific Consulting).....	18
Figure 2.4: Water contact angle of samples with various treatment processes (Sakairi and Goyal, 2016).....	20
Figure 2.5: Anodization Process Diagram (Burns, 2018)	22
Figure 2.6: Schematic Diagram of Cross-Sectional Area of Aluminium Oxide Nano-Porous (Poinern et al., 2011).....	24
Figure 2.7: Formation of Aluminium Oxide Nano-porous layer	25
Figure 2.8: (A) Schematic diagram of the pores formed which is packed ideally in hexagonal array; (B) Typical cross-sectional view of anodic aluminium nano-porous formed from anodization (Parkhutik, et al., 1990).....	25
Figure 2.9: Chemical Half Reaction for Formation of Aluminium Oxide Nano-Porous (Abrahami et al., 2017)	29
Figure 2.10: Bright field TEM micrograph showing typical microstructural variations in specimens of Al alloys: (a) AA2024-T3 and (b) AA7075-T76 (Li et al., 2015).	31
Figure 2.11: Schematic polarization curve for corroding metal, Fe (Corrscience.com, 2011)	35
Figure 2.12: Anodic polarization of aluminum in different electrolyte solutions (Fan et al., 2015).....	36
Figure 2.13: Effect of annealing temperature on hardness of 7075 aluminum alloy (Fallahi, Hosseini-Toudeshky and Ghalehbandi, 2013).....	39
Figure 3.1: Flow of Research Study	41
Figure 3.2: AA7075-T6 samples cut into size of 15 mm × 15 mm × 2 mm.....	42
Figure 3.3: Grinding Machine.....	43

Figure 3.4: Experimental equipment to carry out anodization treatment process for producing aluminium oxide nano-porous arrays	45
Figure 3.5: Power source of direct current (12V) used in the experiment.....	45
Figure 3.6: Set up of electrodes for electrochemical process	46
Figure 3.7: Machine used to conduct scratch test	49
Figure 3.8: Vickers microhardness testing machine	50
Figure 4.1: Anodized surface of AA7075 sample.....	53
Figure 4.2: Schematic diagram of anodization treatment process	54
Figure 4.3: XRD profiles of the (a) substrate, (b) the anodized sample, and (c) the heat treated sample at 450 °C for 1.5 h.....	55
Figure 4.4: Top view FESEM images of series 7 as a substrate.....	57
Figure 4.5: FESEM cross-section images of Al ₂ O ₃ Nano-porous Arrays anodized for 1 h at 12 V in an electrolyte containing 15 wt% H ₂ SO ₄	58
Figure 4.6: Top view FESEM images and (b) EDX of Al ₂ O ₃ Nano-porous Arrays after anodization	59
Figure 4.7: (a) The optical micrograph of scratch track and profiles of (b) depth, (c) load, (d) friction and (e) COF against scan distance after anodization.....	62
Figure 4.8: (a) optical micrograph of scratch track and graphs of (b) depth, (c) load, (d) friction, and (e) COF versus distance for the anodized sample after thermal treatment at 450 °C.	63
Figure 4.9: The variation of Vickers hardness value of substrate, anodized in sulphuric acid and heat treated sample at 450°C.	65
Figure 4.10: Polarization plots of the bare substrate, the aluminium oxide as-anodized specimen, and the 450 °C heat treated sample.....	67
Figure 4.11: (c) heat-treated sample at 450°C.	69

LIST OF TABLES

Table 2.1: Wrought Aluminium Alloy Designation (J. Davis, 1994).....	8
Table 2.2: Aluminium alloy temper designation	11
Table 2.3 : Comparison of Standard Anodizing and Hard Anodizing.....	23
Table 2.4 : Comparison of barrier type and porous type oxide layer formed during.....	27
Table 2.5 : Applications of anodized aluminium alloys in industrial	30
Table 2.6: Classification of Aluminium Alloys Intermetallic Phases.....	32
Table 4.1: Corrosion potential (E_{corr}), corrosion current density (I_{corr}), corrosion rate and effectiveness of corrosion protection ($P.E.$) values.....	68

University of Malaya

LIST OF SYMBOLS AND ABBREVIATIONS

AA	:	Aluminium Alloy
Al	:	Aluminium
Cl	:	Chloride
COF	:	Coefficient of Friction
Cr	:	Chromium
Cu	:	Copper
E _{corr}	:	Corrosion Potential
EDX	:	Energy Dispersive X-ray spectrometry
Fe	:	Iron
FESEM	:	Field Emission Scanning Electron Microscope
H ₂ O	:	Moisture
H ₂ SO ₄	:	Sulphuric Acid
HSp	:	Scratch Hardness
I _{corr}	:	Corrosion Current Density
Mg	:	Magnesium
Mn	:	Manganese
NaCl	:	Sodium Chloride

O ₂	:	Oxygen
PE	:	Corrosion Protection
PVC	:	Polyvinyl Chloride (PVC)
SCE	:	Saturated Calomel
Si	:	Silicon
Ti	:	Titanium
XRD	:	X-ray diffractometry
Zr	:	Zirconium

University of Malaya

LIST OF APPENDICES

Appendix A: Fracture Elongation of metal and its alloys	75
Appendix B: Heat Treatable Aluminium Alloy Temper Designations.....	76
Appendix C: Mechanical Properties of Commercial Aluminium Alloys... 	77

University of Malaya

CHAPTER 1: INTRODUCTION

1.1 Overview

Aluminium with purity that exceeds 99.99% in purity was first available at the early 1920, produced by Hoopes electrolytic process (Hatch, 1984). In year of 1938, a paper on Aluminium properties with 99.996% purity that produced with modified Hoopes process is published in France (Taylor et al., 1938). Moving on with technologies, Hoopes process is replaced by zone-refining technique to obtain higher purity aluminium. Production and properties of the high purity aluminium have been discussed in many papers in the past decade. The Aluminium Association has conducted statistics study on the aluminium demand in Year 2016 and 2017 as shown in Figure 1.1.

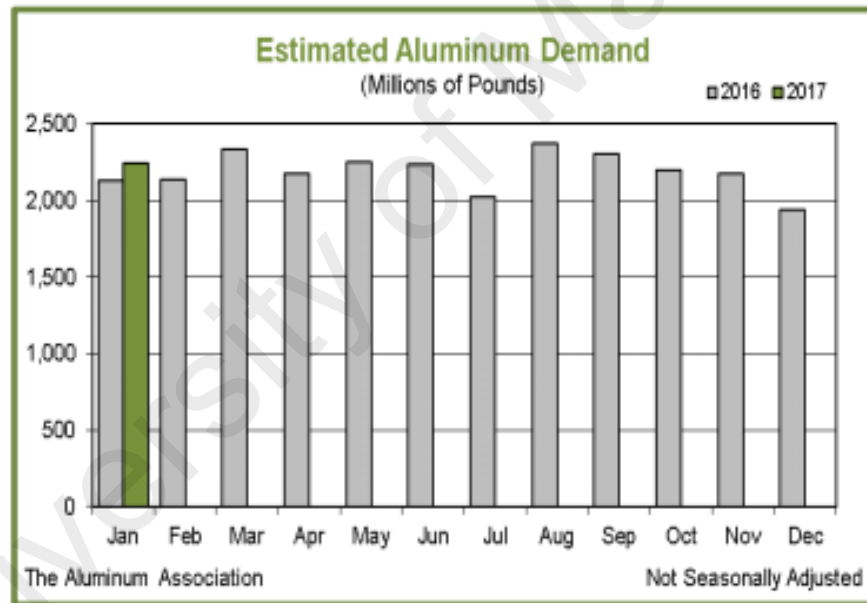


Figure 1.1: Estimated Demand of Aluminium in Year 2016 and 2017 (Villegas, 2017)

According to the statistically preliminary estimation of aluminium demand that published by The Aluminum Association, there is total estimation of 2,242 million pounds of aluminium demand in January, 2017. For years to come, more aluminium alloys will be demanded in the market. Aluminium industry is expanding since late 1800s in production. It has key characteristics of relatively low density which is one third of the

density of steel but have high strength to weight ratio that higher than many constructional steels with common grades. With this advanced property, aluminium is chosen as material and designed into automotive industry as well as aircraft (Villegas, 2017).

In addition, aluminium exhibits flexibility of machining characteristics. It is easily fabricated into desired shape to fit in certain applications and able to be joined by all kinds of joining methods: welding, brazing, riveting or soldering. Aluminium also offers benefit of combining certain key property for specific end users. This included aluminium with high corrosion resistance and thermal conductivity to be embedded in the application of equipment at the petrochemical industries. Despite all these, aluminium is not prone to corrosion. Its material properties will degrade over time under certain environment.

Material degradation of materials have always been one of the major concerns in material engineering study in various structural applications. Researchers study on material behaviors succumbed to different environment factors such as pH, humidity, temperature, salt content. Corrosion is associated with degradation where the relevant properties of material is losing gradually in continuous exposure to the corrosive surrounding (Foley, 1986).

Materials development leads the development of aluminium alloys to another stage in various applications through surface treatment and corrosion prevention techniques. Among the techniques that have been accomplished are plating, anodizing and coating: pre-coating, electro-deposition coating and undercoating. One significant way to prevent corrosion in aluminium alloys is surface modification (Talbot, 2018). It can be done by anodization treatment process and heat treatment. Electrochemical anodization technique able to protect the surface of material from corrosion by forming aluminium oxide nanoporous layer on substrate (Nielsch et al., 2000). Furthermore, heat treatment aims to

improve the surface hardness of the aluminium alloys and protect the surface from the risk of corrosion (Zhecheva et al., 2005).

1.2 Problem Statement

Aluminium industry was undergo rapid growth in production since Charles Martin Hall introduced technology of extracting aluminium from its ore which is electrolytic reduction of aluminium oxide dissolved in molten cryolite. Aluminium offers benefits of flexibility to be engineered in order to fit certain applications by choosing the suitable alloying elements and produce aluminium alloys. Furthermore, its mechanical properties can be improved by tempering and other fabrication process such as surface modification techniques, heat treatment, cold working and etc. However, there is high potential for aluminium undergoes corrosion when aluminium is being exposed to particles or corrosive environment. Self-protecting oxide layer will be destroyed and surface of aluminium will be degraded.

Corrosion of aluminium is associated with flow of electric current between various anodic and cathodic regions (McCafferty, 2010). Hence, surface modifications are proposed to improve the material properties of aluminium alloys in order to enhance the corrosion resistance. In this current study, aluminium alloy is anodized and undergo heat treatment in order to improve its corrosion properties. Prior to this research work, not much information was reported on the characterization of surface modification on corrosion resistance of aluminium alloy series 7. Little attention has been paid to strengthening the aluminium alloy series 7 through both anodization and heat treatment. Hence, from this study, corrosion behavior of aluminium alloy series 7 can be justified and compared after being anodized and heat-treated.

1.3 Objective

The current research project attempts to look into the corrosion behavior of aluminium alloys and effects of surface treatments on corrosion properties. The work focuses on formation of aluminium oxide nano-porous arrays through anodization as well as heat treatment of aluminium alloy series 7075. Objectives have been set in this research project:

- a) To fabricate aluminium oxide nano-porous layer by application of surface modification, which is anodization and heat treatment.
- b) To investigate the corrosion behavior of aluminium alloy 7075 and effect of surface modification on its corrosion behavior through experimental methods and microstructure analysis.

1.4 Scope of Study

This study mainly focuses on the corrosion study of aluminium alloy series 7075 that applied surface finishing techniques which is anodizing and heat treatment. The aluminium alloy series 7075 samples undergoes DC anodizing in a sulphuric acid electrolyte in order to form aluminium oxide nano-porous arrays. Aluminium nano-porous arrays and heat treated aluminium alloys series 7075 are characterized in terms of its microstructure and phase composition. Mechanical properties of aluminium oxide nano-porous and substrate is compared which including adhesion strength, wettability and microhardness. Corrosion studies are conducted in this study in order to investigate the corrosion behaviours of the alloy before and after surface modification. Flow of research activities is summarized in flow chart shown in Figure 1.2

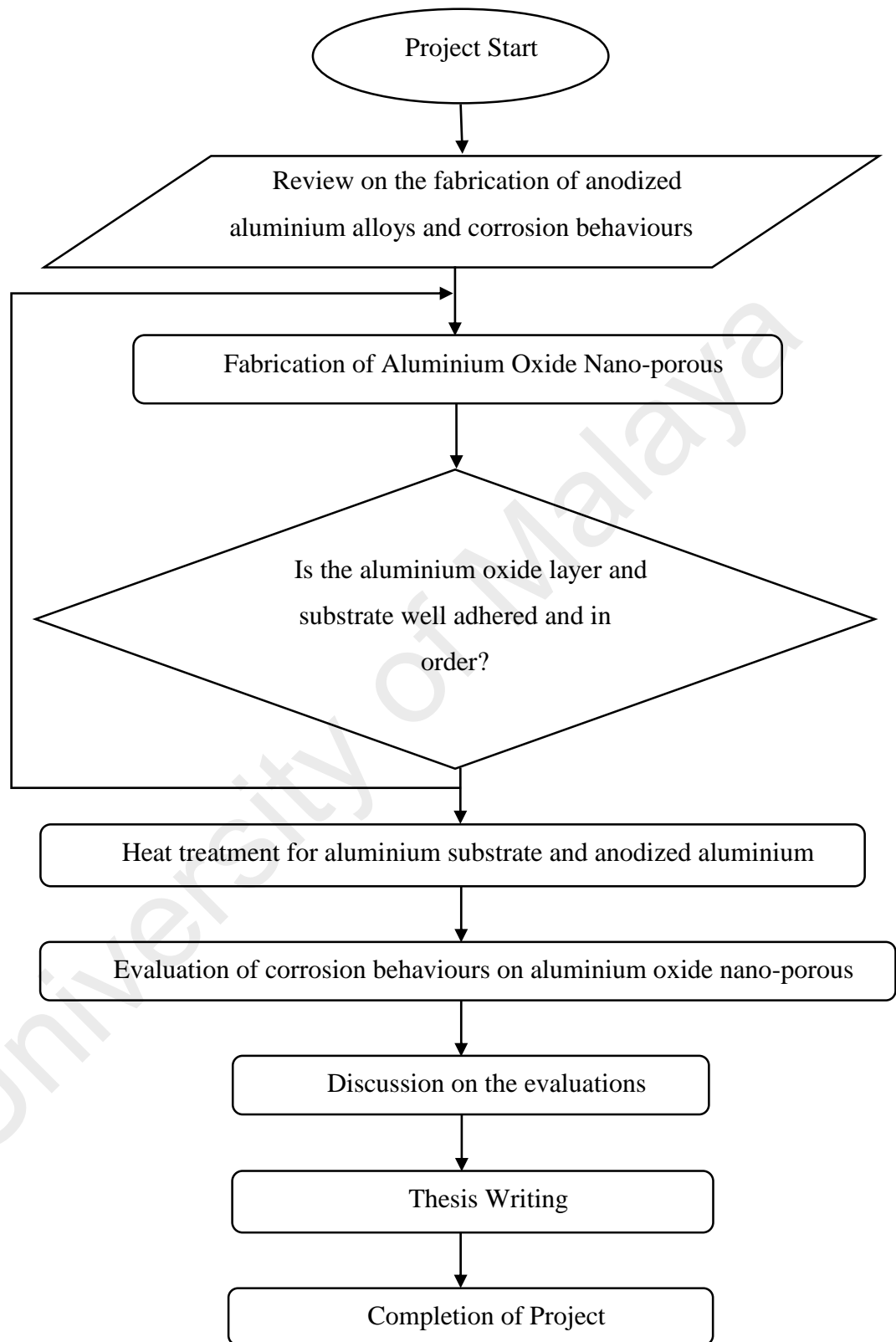


Figure 1.2: Flow of Research Study Activities

CHAPTER 2: LITERATURE REVIEW

2.1 Aluminium and Aluminium Alloys

Aluminium has atomic weight is 26.98g/mol and with atomic number of 13. The strength of pure aluminium decreases as the purity increases, however its ductility increases. In nature, aluminium is soft, its alloys are widely used automotive applications, such as materials for heat insulators, pistons, compressor wheels and rotors, interior body panels and etc. Aluminium alloys series 3000 (Aluminium-Manganese), 5000 (Aluminium-Magnesium) and 6000 (Aluminium-Magnesium-Silicon) exhibit good corrosion resistance (Miller, *et al.*, 1938).

Aluminium is prone to corrosion, however it will undergo oxidation when it is exposed to surrounding atmospheric oxygen. As a result, a thin film of aluminium oxide will form which act as a protective layer that halt aluminium corrosion process.

Protection of aluminium is required as it is active component in order to be used in various applications. In the mid of 1920s, anodization process is introduced and refined actively as its applications in industry increased in demand (G.E.,Thompson, 1997). Studies and researches were widely conducted to venture into anodizing techniques and material properties of anodized aluminium alloys.

2.1.1 Aluminium Alloy Designation

Series number is designed to the aluminium alloy for the purpose of categorization in term of easing the application in which the alloy is most suited. Every series of aluminium alloys exhibits distinct material characteristics as selection of materials to fabricate products in the industry. For instant, aluminium alloy series 1xxx is commonly adopted in the application of high-level electrical conductivity, such as high-power electrical lines. Aluminium alloy in series 2xxx are practically used in application that needs strengthened properties. In some cases, series 2xxx aluminium alloy are used together with series 6xxx aluminium as protected by the external coating layer for protection purpose (Schuman, 2018). Most of the automotive applications adopted aluminium silicon alloy, which is series 4xxx alloys whereas series 7xxx aluminium alloys is significantly chosen for implementation in aircraft applications. Figure 2.1 shows the aluminium alloy designation tree that illustrates the examples of aluminium alloy in each series and its applications.

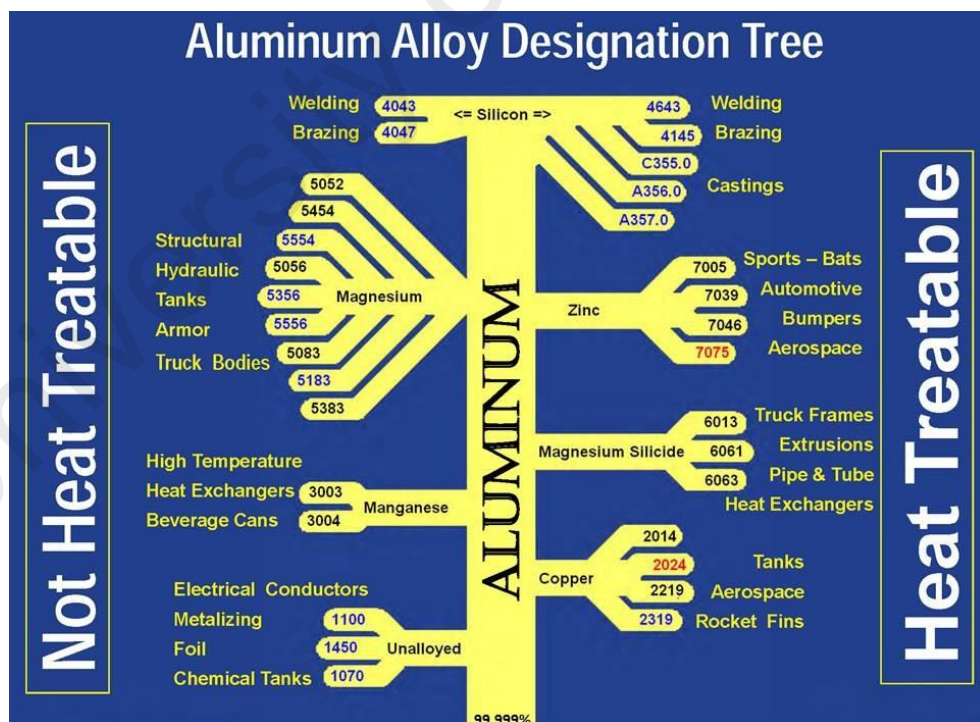


Figure 2.1: Application of Aluminium Alloys (Burns, 2018)

In the 4-digit wrought alloy designation system for aluminium alloy, first digit of the alloy series represents the principal alloying element in the aluminium alloy, which also used to describe the aluminium alloy series from alloy 1000 series until 8000 series. For example, alloy series 1xxx comprises of 99.000% minimum aluminium; alloy series 2xxx has principal alloying element of copper and so on. Second single digit indicates modification of specific alloy. For aluminium alloy with second digit other than zero, modifications have been made in order to improve the ductility and strength of aluminium alloy for example, strain or thermal hardening.

Third and fourth digits of the aluminium alloy are given to ease the identification of specific alloy in the particular series. In this research project, aluminium alloy series 7xxx, AA7075-T6 is studied. First digit which is 7 (i.e. AA7xxx) means that the alloy contains element of Zinc (Zn). Second digit of zero (i.e. AAx0xx) indicates that there is no modification of the specific alloy whereas third and fourth digit (xx75) identifies it in the 7xxx series. Principal alloying element of aluminium for different series is summarized in the Table 2.1.

Table 2.1: Wrought Aluminium Alloy Designation (J. Davis, 1994)

Alloy Series	Principal Alloying Element
1XXX	99.000% Minimum Aluminium
2XXX	Copper
3XXX	Manganese
4XXX	Silicon
5XXX	Magnesium
6XXX	Magnesium and Silicon
7XXX	Zinc
8XXX	Other elements

Aluminium in series 1xxx has significant characteristics of excellent resistance towards corrosion, high thermal and electrical conductivity. It is used widely for applications of electrical. Its mechanical properties can be improved by strain hardening. The major alloying elements are iron and silicon. Among the alloys from Series 1xxx are 1050, 1060, 1100, 1145, 1200, 1350 and so on.

Major alloying element in aluminium series 2xxx is copper. It is commonly adopted in aircraft construction and suitable for the manufacturing of parts that need to meet the acquired strength at high temperature of 150°C. In order to achieve optimum mechanical properties, aluminium alloy series 2xxx has to undergo solution heat treatment. In addition, aging or precipitation heat treatment also used to improve the aluminium alloy series 2xxx mechanical properties, such as yield strength. Example of aluminium alloy series 2xxx are 2011, 2014, 2017, 2018, 224.0 etc. Compared to other series of aluminium alloy, Series 2xxx has poorer corrosion resistance and it is exposed to the risk of intergranular corrosion in certain environment conditions (Glanvill, 2018).

In general, aluminium alloy series 3xxx are non-heat treatable, having limited manganese as its principal alloying element which is up to approximately 1.5%. Aluminium alloy 3xxx series such as 3003 and 3004 are normally used to produce beverage can in canning industry.

Aluminium alloy series 4xxx are normally used as material to produce welding wire and brazing alloys for aluminium joining due to its low melting range, for instance AA4043. The presence of silicon in aluminium alloy series 4xxx causes the property of having low melting range than the base metal required.

Aluminium series 5xxx such as 5052, 5083, etc. exhibits good corrosion resistance and weldability. Thus, it is suitable for marine applications as it can slow down the corrosion rate due to reaction of metals with the marine atmosphere. Magnesium is the major alloying element in aluminium alloy series 5xxx, in the way that 0.8% of magnesium is

comparable to 1.25% of manganese. However, magnesium content should be limited to 3% or less in order to avoid stress-corrosion cracking. For petrochemical and refinery plant that located nearby the sea, aluminium alloy series 6xxx is commonly chosen as the materials to construct tank platform or railing.

Aluminium alloy series 6xxx is heat treatable as it comprises silicon and magnesium that able to form magnesium silicide (Mg_2Si). Having advantage of good formability in shaping as well as weldability, aluminium alloy series 6xxx such as AA 6061 is used widely in extrusion. Furthermore, aluminium alloy series 6xxx possess good corrosion resistance and heat-treatable make it a selective raw material for fabricate pipe and tube of heat exchanger. Similar to aluminium alloy series 6xxx, content of silicon and magnesium added in the alloy should be controlled in order to prevent formation of magnesium silicide that will lead to intergranular corrosion (Tavares et al., 2015).

Aluminium alloy series 7xxx is used in the applications that required high stress intensity, for instance airframe structures, automotive, vehicle bumpers, etc. Zinc is the main principal alloying element, with small portions of magnesium and copper added. Among the aluminium alloys, aluminium alloy series 7xxx has the highest strength. In spite of high tensile strength, its resistance towards corrosion is reduced. Optimum combinations of aluminium alloy series 7xxx mechanical properties (tensile strength and fracture toughness) and corrosion resistance can be achieved in utilization to some degree of overaged temper. Example of aluminium alloy series 7xxx that having highest strength is AA7075 which is typically used in aerospace applications (Santa et al., 2015).

Aluminium series 8xxx is allocated for the alloying elements that are not in the classification of series 2xxx to 7xxx. For instance, alloying elements of iron and nickel is added to aluminium alloy 8017 which is conductor alloys by maintaining its electrical conductivity.

2.1.2 Temper Designation of Aluminium Alloy

With regards to the alloy designation of aluminium alloy, basic treatments that have been applied to fabricate different classes of aluminium alloys are represented by using temper designation. The summarized the aluminium alloy temper designation is shown in Appendix 1.

Table 2.2: Aluminium alloy temper designation

Temper Designation	
F	As fabricated, amount of strain hrdening is out of controlled, no limitations on mechanical property
O	Heat treated and recrystallized. Temper with lowest strength and highest ductility
H	Strain hardened
T	Heat-treated to produce stable tempers
Stain-hardened subdivisions:	
H1	Strain hardened only. The degree of strain hardening is shown by the second digit and differ from quarter hard (H12) to full hard (H18) that produced through area reduction of approximately 75%
H2	Partially annealed and strain hardened. Temper is ranging from quarter hard (H12) to full hard (H18) achieved by annealing partially of cold worked materials with strength initially greater than desired. Tempers are H22, H24, H26 and H28.
H3	Strain hardnened and stabilized. Tempers for age-softening Al-Mg alloys that are strain-hardened and then heated at low temperature to increase ductility and stabilized the mechanical properties. Tempers are H32, H34, H36 and H38.
Heat-treated subdivisions:	
W	Solution treated
T	Age hardened
T1	Cooled from fabrication temperature and naturally aged
T2	Cooled from fabrication temperature, cold-worked and naturally aged
T3	Solution-treated, cold-worked and naturally aged
T4	Solution-treated, cold-worked and naturally aged
T5	Cooled from the fabrication temperature and artifically aged
T6	Solution-treated and artifically aged
T7	Solution-treated and stabilised by over-ageing

T8	Solution-treated, cold-worked and artificially aged
T9	Solution-treated, artificially aged and cold-worked
T10	Cooled from the fabrication temperature, cold-worked and artificially aged

2.1.3 Electrochemistry of Aluminium

A thin, invisible adherent oxide film which acts as a natural protection layer to aluminium makes it has high resistant towards corrosion. It is formed the moment aluminium is exposed to oxygen (reference) with thickness of approximate 3-5nm. However, the native oxide layer formed is unable to resist the corrosion when aluminium is under the exposure of harsh surrounding such as acidic, high temperature and so on. Factors contribute to the corrosion of aluminium is further discussed in the Chapter 2.2.2.

Corrosion resistance of aluminium can be improved by applying surface treatment techniques. Alloying is the most common and basic method to prevent corrosion of aluminium. Hence, aluminium alloy with various alloying elements are used widely in the global market applications. Microstructure and heterogeneity of aluminium alloys are different from each other (Hannard et al., 2016). Meanwhile, localized corrosion might be taken place in aluminium alloys under certain circumstances.

Copper is known for having lower corrosion resistance compared to the other alloying elements whereas magnesium does not really improve the corrosion prevention in aluminium. Thermal treatments conducted will alter chemical properties of aluminium alloys and affect the localized corrosion resistance due to the change in microstructure of aluminium. Practically, corrosion resistance of aluminium alloys is lowered with localized microstructural effect via electrochemical heterogeneity (Kairy, 2016).

In some aluminium alloy series especially those with magnesium content of more than 3% (2xxx, 5xxx, 7xxx), there is higher potential to undergo corrosion such as

intergranular attack, exfoliation and stress-corrosion cracking. Based on the past studies, aluminium alloy that consist of Zinc and Magnesium as major alloying element has highest susceptibility towards stress-corrosion cracking. Aluminium alloy series 7xxx which is considered as high-strength aluminium alloy also prone to hydrogen embrittlement.

2.1.4 Aluminium Alloy 7075 Properties

In aluminium alloy series 7, Zinc (Zn) is the major alloying element. This series of alloy exhibits good mechanical properties. Aluminium alloy 7075 has the highest grade in the aluminium alloy classification. Either aluminium alloy 7075-O or 7075-T6 is used for the application of aviation (as raw material of bearing and landing gear fabrication), rocket, propeller, air vehicle and etc. It is used extensively in aviation application due to its ability to offer significant weight reduction. In market, many existing products are made from aluminium alloy, for example there are some components in the Apple Watch are made of aluminium alloy 7075 variant (Quora.com, 2018). However, aluminium alloy AA7075 has its limitations which are poor tribological properties and susceptible to localized corrosion as it has tendency to adhesion is high and has lower hardness.

Localized corrosion of aluminium alloy 7075 is studied widely by researchers over the ages. It is susceptible to localized corrosion such as pitting, exfoliation or intergranular corrosion that potentially results from inter-metallics distribution, type and concentration factor as well as the strengthening materials. Strengthening materials of aluminium alloy 7075 consists of $MgZn_2$ that in the size of nanometers. During heat treatment process, precipitation takes place in these particles along the grain boundary. Compared to the matrix, the strengthening particles are more active electrochemically, hence high chances of causing intergranular corrosion (Liu, Mol and Janssen, 2016).

Electrochemical reactivity of the main inter-metallics, $\text{Al}_7\text{Cu}_2\text{Fe}$ and $(\text{Al}, \text{Cu})_6$ (Fe, Cu) is less than the matrix. Hence, it will cause dissolution of the surrounding regions (12). There is possibility of chemical reaction to take place between the base materials which is AA7075 and its matrix, thus might cause galvanic coupling (Pao PS, Feng CR, Gill SJ, 2000). Iron (Fe) and copper (Cu) are the main inter-metallics in aluminium. Material characterizations of inter-metallics and strengthening particles have been studied with microscopy such as Scanning Kelvin Probe Force Microscopy (SKPFM) or through micro-capillary studies (Liu, Mol and Janssen, 2016).

Zinc is able to increase the electrode potential of aluminium substantially. Therefore aluminium-zinc alloys are used widely for the application of alclad coatings.

2.2 Overview of Corrosion

Deterioration of material, which commonly takes place in metals and alloys due to the chemical or electrochemical reaction with environment is known as corrosion (F.N. Speller, 1951). In 1819, an anonymous French writer who thought to be Thenard described that corrosion is an electrochemical phenomenon in a paper published (Ulick, 1948). This phenomenon occurs naturally with the environmental factors for example soil resistivity, humidity, salt water exposure on different types of metals. Besides, corrosion phenomenon also influenced by the nature of the metal or its properties such as homogeneity and electrochemical activity of the material. Apart from that, physical conditions which including design, temperature, electrolyte concentration, potential of the electrode and mechanical action affects corrosion too (Corrosion-doctors.org, 2018).

There are three theories of corrosion: acid theory, dry or chemical corrosion and galvanic or electrochemical or wet theory of corrosion. Acid theory expresses that presence of acids at the surrounding of a metal (refer to iron) causes corrosion. Carbon dioxide, oxygen and moisture in the atmosphere are the main elements that caused

corrosion in iron based on this theory. Corrosion product consists of iron hydroxide and carbon dioxide. It is supported by the analysis of rust that tests on the presence of carbon dioxide ion. According to dry or chemical theory of corrosion, direct reaction of atmospheric gases such as oxygen, halogens, oxides of sulphur, oxides of nitrogen, hydrogen sulphide and fumes of chemicals with metal surface will lead to corrosion. Dry corrosion comprises of three main types which are: oxidation corrosion, corrosion due to corrosive gases and liquid metal corrosion. Wet or electrochemical theory of corrosion takes place when the metal comes in contact with a conducting liquid or when two dissimilar metals are immersed or dipped partly in a solution (electrolyte). One of the metals will act as anode while another act as cathode. Flow of electrons formed galvanic cell. Oxidation half reaction takes place at the anode results in corrosion and reduction takes place at cathode simultaneously. Corrosion product will be deposited on the metal surface in between of anode and cathode.

The significant difference between dry corrosion and wet corrosion is that dry corrosion occurs in the absence of moisture while wet corrosion occurs in presence of conducting medium. Wet corrosion takes place more rapidly compared to dry corrosion. Other than that, corrosion products are formed at the site of corrosion when dry corrosion takes place. In wet corrosion, corrosion takes place at the anode but the rust is deposited at the cathode.

2.2.1 Types of Corrosion

Basically, there are ten primary forms of corrosion which can be categorized in three main groups by distinguishing the appearance of the corroded surface. Group I type of corrosion is readily justified through visual examination which including uniform corrosion, pitting, crevice corrosion, galvanic corrosion, filiform corrosion and etc. Corrosion such as cavitation, erosion, intergranular corrosion, dealloying (selective

leaching) and exfoliation requires advanced approaches in order to verify. It is easier to verify the corrosion mechanism through colour changes or formation of brown rust on the surface of the materials.

For Group II type of corrosions, special inspection tools are required for corrosion justifications. Example of the corrosions are erosion, cavitation, fretting and intergranular corrosion. The most common way to conduct Group II corrosion verifications are through tools and related technologies. The corrosion mechanisms will be looked in more detailed and confirmed with the techniques and laboratory equipment.

Types of corrosion fall in the Group III will be examined by using microscopes and related technologies as it is very hard to be justified by naked eyes.

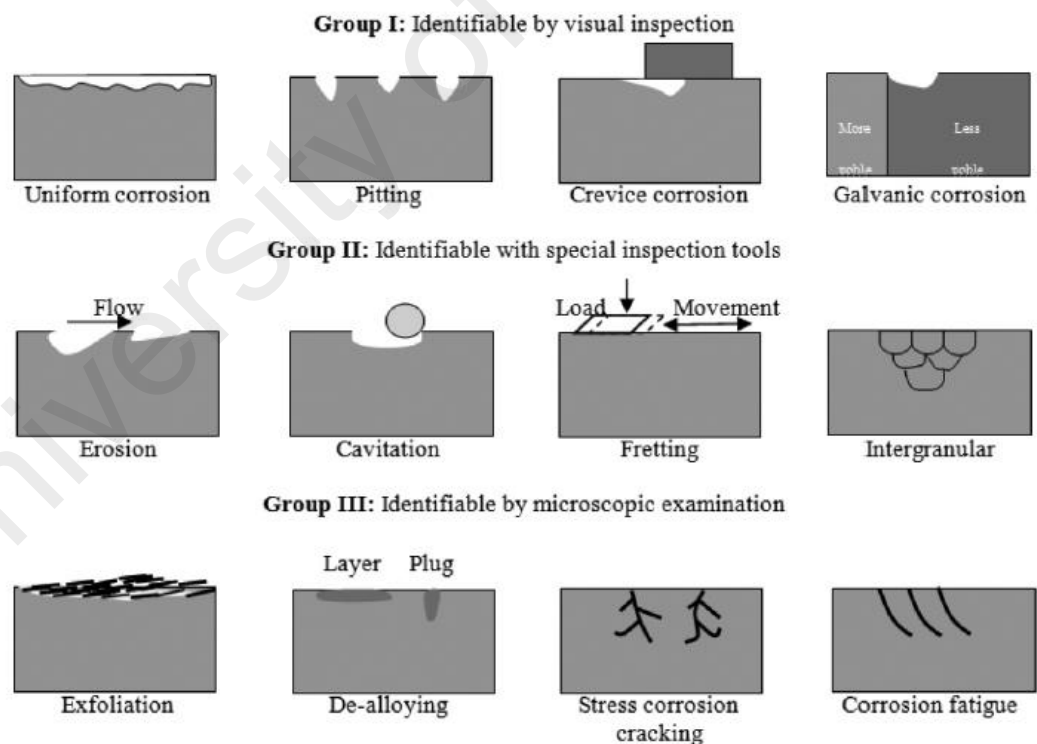


Figure 2.2: Schematic Diagram of Several Types of Corrosion

2.2.2 Corrosion Mechanism of Aluminium Alloy

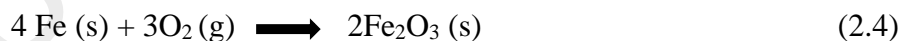
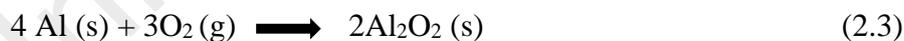
Corrosion of aluminium is closely related with electric current flow between distinct anodic and cathodic regions. Different in potentials of these regions will lead to electrochemical corrosion. General corrosion behavior in aluminium is affected by two major factors which are environment type and its aggressiveness and aluminium materials properties in term of its metallurgical as well as the chemical structure. Aluminium has high tendency to corrode when substances such as sulphates and chlorides are present in the surrounding which is common in industrial and marine.

Anodized aluminium might undergo corrosion if the coating is not well adhered to the aluminium substrate over some duration of exposure to harsh surrounding. In the presence of Chloride (Cl^-), Oxygen (O_2) and moisture (H_2O), chemical reaction will take place with the aluminium oxide or coating on the adjacent to aluminium surface. The chemical reaction can be represented by the half chemical reaction equations below:

Half chemical reaction equation at the anode:



Half chemical reaction equation at the cathode:



Fe_2O_3 is the rust that formed on the aluminium surface after reacts with oxygen. The corrosion mechanism is illustrated in Figure 2.3.

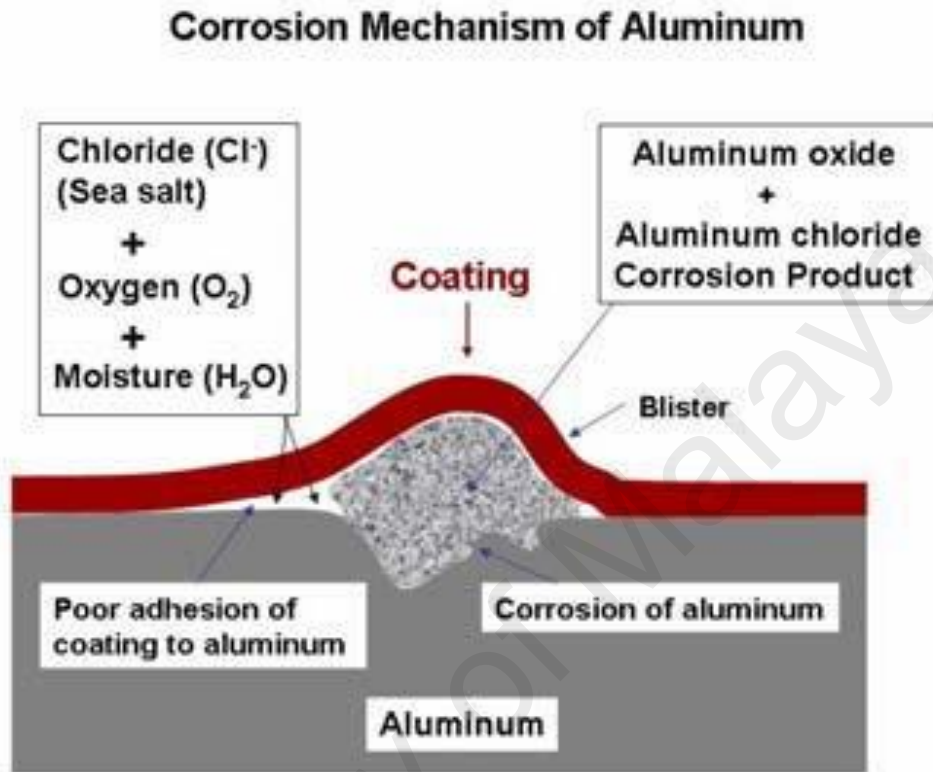


Figure 2.3: Mechanism of corrosion in coated aluminium (source: Exponent Engineering and Scientific Consulting)

In nature, aluminium cannot exist in the form of free state as it is extremely reactive element that having strong reactivity towards oxygen. Aluminium will undergo oxidation immediately under exposure to the air and it corrodes. When aluminium contacts directly with other material, it tends to corrode. In some cases, rubber or Polyvinyl Chloride (PVC) sheet is used as material separator in between aluminium and the materials in contact with.

In case there is limited space to locate the material separator, painting is applied on the dissimilar materials such as steel in order to avoid corrosion when contact directly with aluminium alloy. Alternatively, priming paint that does not contain lead with good quality can be applied on the steel surface that need to be used contact directly with plain

aluminium. Furthermore, painting also applied to the copper or any other types of heavy metal exposed to the air that in contact directly with aluminium. Either aluminium or the material in contact with, such as steel and copper can be coated or painted. Sealant also can be applied on the faying surface as an additional protection to the materials when severe corrosion is distinguished.

Corrosion takes place with the presence of water or moisture and oxygen in the surrounding. It is important to take note on the materials in contact with aluminium for any applications. In particular, materials that has good absorption of water and porous surface property such as woods, fiber board water shall not be located directly with aluminium. However, it can be overcome by installing an insulating barrier at the interface of aluminium and porous materials.

In short, direct contact between two dissimilar materials shall be avoided during engineering design especially for the applications subjected to the harsh corrosion surrounding. Designs of the structures of materials is very crucial in order to minimize the risk of corrosion of aluminium by knowing the material properties in contact with.

2.2.3 Corrosion Resistance and Hydrophobicity Mechanism

Metal with surface of big water contact angle is defined as hydrophobic surface. As the water contact angle increases, the wettability of the material will decrease relatively. Low wettability materials are highlighted to be adopted in application such as petroleum industry, architecture, shipbuilding and other industries. Microstructure is more crucial compared to chemical composition in mechanism of hydrophobicity. The main criteria of reducing surface wettability is by forming fine, ordered and regular porous surface.

Lowering of aluminium surface wettability can be achieved by using anodizing and desiccation treatment through the formation of surface hydrophobicity (Zheng et al., 2010). Figure 2.4 demonstrates the water contact angle of specimens that treated with different processes. Anodized specimens either unpolished or polished show low water contact angle whereas anodized specimens subjected to desiccation treatment exhibit high contact angle. From the findings, majority of surface with high water contact angle surface or generally known as hydrophobic surface formed through organic chemical coating with diminish its hydrophobic property after being anodized in aqueous solution (Sakairi and Goyal, 2016).

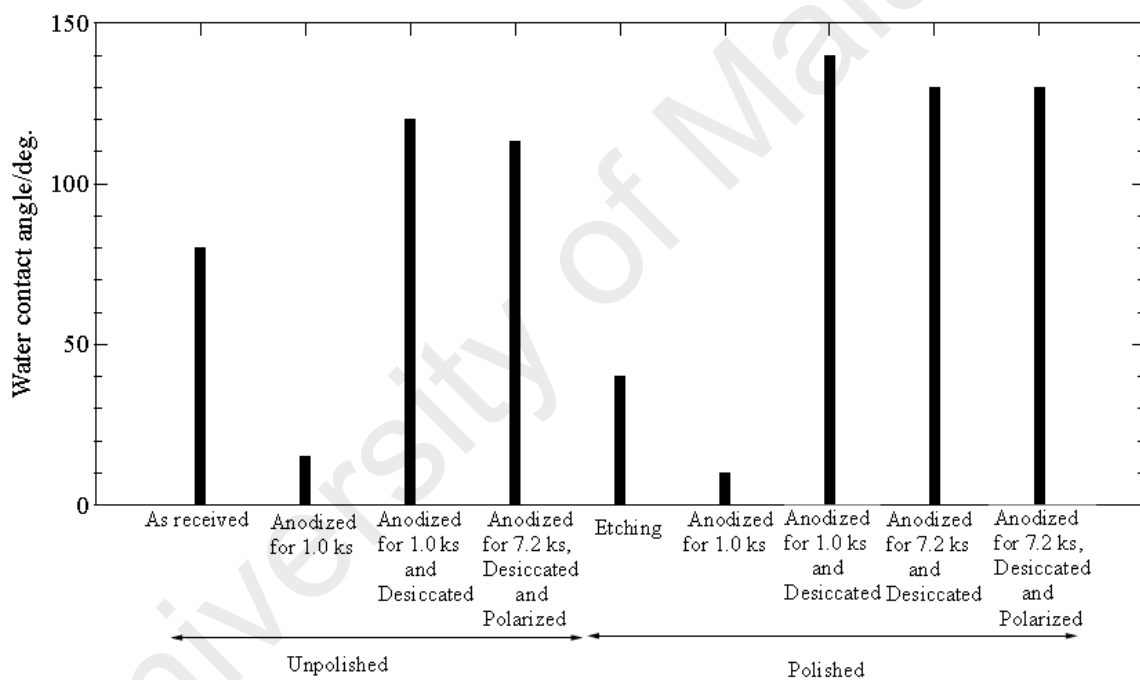


Figure 2.4: Water contact angle of samples with various treatment processes (Sakairi and Goyal, 2016).

Desiccation treatment is carefully conducted with anodization in order to increase the water contact angle, reduce the surface wettability by formation of ordered pore structure. In fact, small amount of water is presence in porous oxide layer formed during anodization. Through microscopic observation, the porous oxide layer consists of many pores in cylindrical tube shape at where capillary action takes place with solution at the interface. However, the solution will not reach the bottom of pores as air-valley will

forbid it. Air trapped inside the cylindrical tube acts like air-valley. This phenomenon can be explained by the surface tension and air pressure trapped to support water droplet from penetrating to the pore bottom (Zheng et al., 2010). Hence, the surface wettability is greatly reduced through desiccation treatment by decreasing metal dissolution rate in solution. As a result, the corrosion resistance is improved.

2.3 Surface Modification of Aluminium Alloy

Surface treatment and surface coatings are common alternatives in prevention of corrosion. In the current research project, anodizing and surface treatment are in the area of interest to be studied. Anodizing is further discussed in the sections below.

2.3.1 Anodizing of Aluminium-metal Oxide Composite

Anodizing process is a reinforcement of oxide process that occurs naturally that most commonly used in aluminium and aluminium alloy. It is an application to improve the metal corrosion resistance and wear resistance through formation of oxide layer on the metal surface, which is highly controlled oxidation process. This surface treatment method allows the thin oxide layer formation by undergoing an electrochemical process. Unlike coating or plating, aluminium oxide is a reacted finish that fully integrated with the underlying aluminium substrate in order to achieve total bonding and unmatched adhesion.

Anodizing of aluminium can be achieved through anodizing treatment process that usually carried out in electrochemical cell. It can be easily performed by attaching aluminium sample to the jig to hold it in position. Then, it is immersed in the sulphuric acid or oxalic acid that commonly used as the electrolysis solution or known as electrolyte which acts as charge carriers. In the electrochemical process, aluminium sample acts as anode by connecting electrode to the jig and positive current is applied to it. Simultaneously, negative current will be flow across the cathode. Materials selected for cathode can be aluminium, graphine or platinum. Eventually, a layer of oxide film which is aluminium oxide coating will be deposited on the surface of aluminium sample. Figure 2.5 illustrates the schematic diagram of the anodizing treatment process.

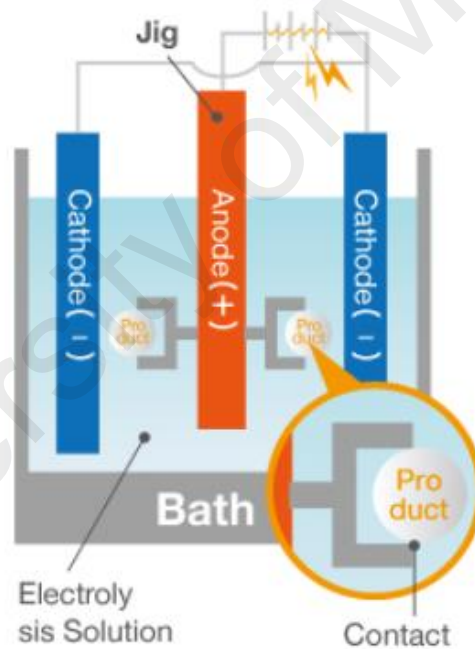


Figure 2.5: Anodization Process Diagram (Burns, 2018)

There are two main types of aluminium anodizing: standard anodizing and hard anodizing. Differences between these two types of anodizing techniques are summarized in the Table 2.3. There is vast development in anodizing processes in order to best suit

the applications of the respective aluminium alloys. Maximum optimization of anodizing is targeted in meeting the functional properties of high-end products.

Conventional anodizing techniques including chromic acid anodizing, sulphuric acid anodizing, organic acid anodizing, phosphoric acid anodizing, barrier type anodizing and plasma electrolytic oxidation (Sheasby and Pinner, 2001).

Table 2.3 : Comparison of Standard Anodizing and Hard Anodizing

	Surface Anodizing (white/colour)	Hard Anodizing
Treatment Overview	Most common treatment method using sulphuric acid as electrolyte	Treatment conducted in low temperature electrolytic bath generates thick, hard film
Colour Tone	Usually white in colour, however colouring can be used to generate desired colour	Naturally has grayish colour that will differ with the type of aluminium and film thickness
Hardness	Approximately 200HV	Greater than 400HV
Film Thickness	Decided by application conditions, usually about 5 μ -25 μ	Generally specified 2 μ -7 μ based on wear resistance, electric insulation properties
Dimensions	Plus ½ film thickness	Plus ½ film thickness
Main Applications	Construction materials, industrial goods, household goods, ornaments	Sliding parts including shaft and rollers, aircraft parts

2.3.1.1 Formation of Aluminium Nano-porous

Pores with sizes of about $10\mu\text{m}$ to $30\mu\text{m}$ in diameter is formed in the oxide films after anodizing treatment process. In fact, formation of pores with 5-70 billion per cubic centimeter is achieved (Kashima-coat.com, 2018). Cross section of the nano porous structure that formed on the aluminium surface is illustrated in the Figure 2.6.

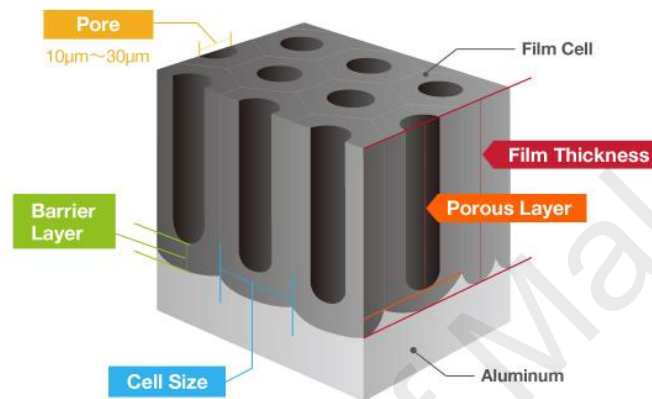


Figure 2.6: Schematic Diagram of Cross-Sectional Area of Aluminium Oxide Nano-Porous (Poinern et al., 2011)

Aluminium nano-porous coating formed has thin inner layer whereas its outer layer is thick. Based on the studies carried out by few researchers, there is finding on nano-porous layer formed is in hexagonal honeycomb structures, which as illustrated in Figure 2.8 (Poinern et al., 2011). Differ from barrier type layer, there is a thin non-porous oxide layer formed adjacent to metal substrate which is with thickness that remained unchanged in porous type oxide layer. It will continuously generated at the bottom of the pore in conjunction with the formation of pore wall. The layer formation is shown in Figure 2.7.

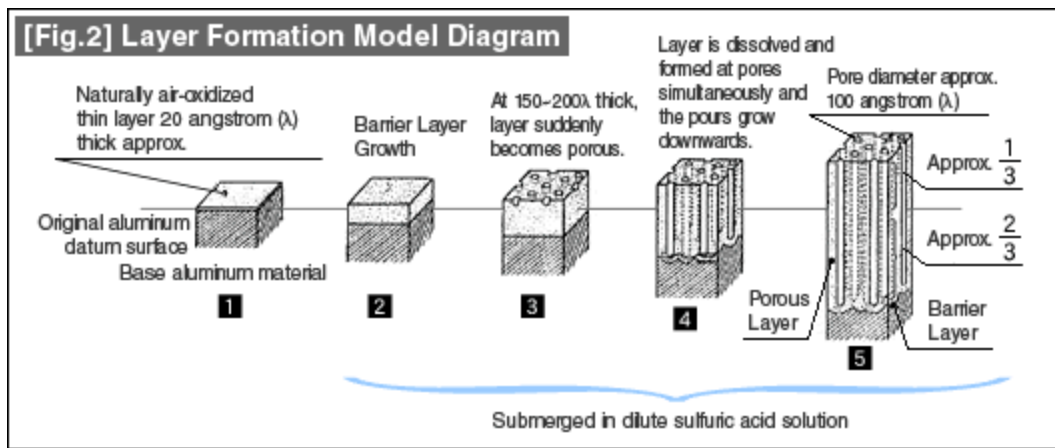


Figure 2.7: Formation of Aluminium Oxide Nano-porous layer

Initially, oxide layer will grow proportional to the anodizing duration and pore patterns will be revealed and started to immerse till it develops in more orderly manner. Pores with long-range structured configuration will be developed in single formed. Figure 2.7 shows the schematic diagram of the pores formed ideally (Parkhutik et al., 1990). In ideal case, the formation of nano-porous from aluminium alloy anodization is with pore density of range from 10^8 to 10^{12} pores per centimeter square (Zhao et al., 2005).

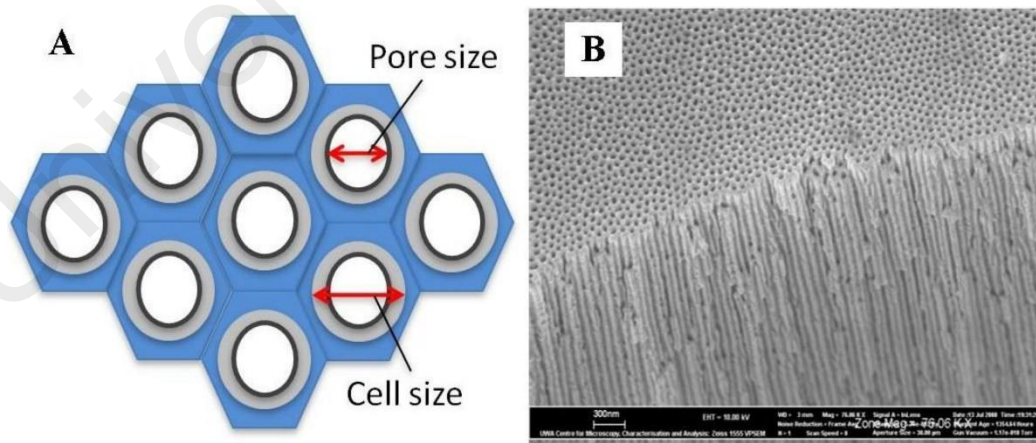


Figure 2.8: (A) Schematic diagram of the pores formed which is packed ideally in hexagonal array; (B) Typical cross-sectional view of anodic aluminium nano-porous formed from anodization (Parkhutik, et al., 1990)

Size of pore formed and the distance between pores in aluminium nano-porous is determined by parameters of anodizing preparation: type of electrolyte used in anodizing treatment process, concentration of electrolytes, anodic voltage applied to the electrode, current density and the bath temperature. The effects of manipulating the parameters of anodization can directly give impact to the structures and characteristics of the pore formed (Melendres et al., 2001).

Formation of the oxide films or anodic films are categorized into two types: barrier type and porous type layer that depends on the type of electrolytes used, which is the primary determinant factor (Prasad and Quijano, 2006). Barrier type oxide films can be formed by using neutral boric acid, ammonium borate or tartrate aqueous baths as electrolyte. Initially, the barrier type oxide films formed are insoluble. On the contrary, porous type layer is slightly soluble formed by using acidic form of electrolytes such as sulphuric acid, chromic acid, phosphoric acid and etc. Several researches carried out studies on the transition of barrier type oxide layer into porous type and there are few theories on pore formation have been proposed. The differences between these two types of anodic oxide films that deposited on the aluminium surface is being outlined in Table 2.4 (Diggle et al., 1969).

Table 2.4 : Comparison of barrier type and porous type oxide layer formed during anodizing process of aluminium (Diggle et al., 1969)

	Barrier Type	Porous Type
Structure	Thin, compact, non-porous	Inner layer- Thin, compact barrier-type Outer layer- Thick and porous
Thickness	Voltage dependent, ~ 1.4nm/V	Inner layer- Voltage dependent, ~ 1nm/V for sulphuric acid Outer layer- Voltage dependent, current density, time and temperature dependent
Typical Electrolytes	Solutions of Boric acid- Borax Citric acid- Citrate Ammonium tartrate	Sulphuric, Phosphoric, Chromic and Oxalic acid aqueous solutions

The mechanism of anodizing reaction can be represented by the following equation:



Aluminium Nano-porous layer formation through dissolution of aluminium:



Cathodic half chemic reaction at the cathode at where hydrogen gas is released:



Anodic half chemical reaction at the anode (metal-oxide interface):



Chemical half reaction at the oxide-electrolyte interface:



Cathodic chemical half reaction at the cathode:



Initially, aluminium (Al^{3+}) ions will migrate from the aluminium substrate into layer of oxide formation (Patermarakis, 1998). Simultaneously, presence of water in electrolyte leads to the formation of oxide ions (O_2) and it will migrate towards oxide layer. The formation of oxide layer is made up of about 70% of the Al^{3+} ions and O_2 formed at this stage (Palbroda, 1995). Entire Al^{3+} ions will be dissolved or as mentioned before, incorporated into the electrolyte solution. Prior to the formation of the aluminium nano-porous, bonding between aluminium and oxygen is broken in the oxide lattice to achieve ionization of aluminium (Shawaqfeh, 1999).

Growth of oxide is continued with the formation of nano-porous oxide layer and eventually it pore bottom with semi-spherical oxide layer with constant thickness is achieved. The chemical reaction of the formation of aluminium nano-porous is demonstrated in Figure 2.8.

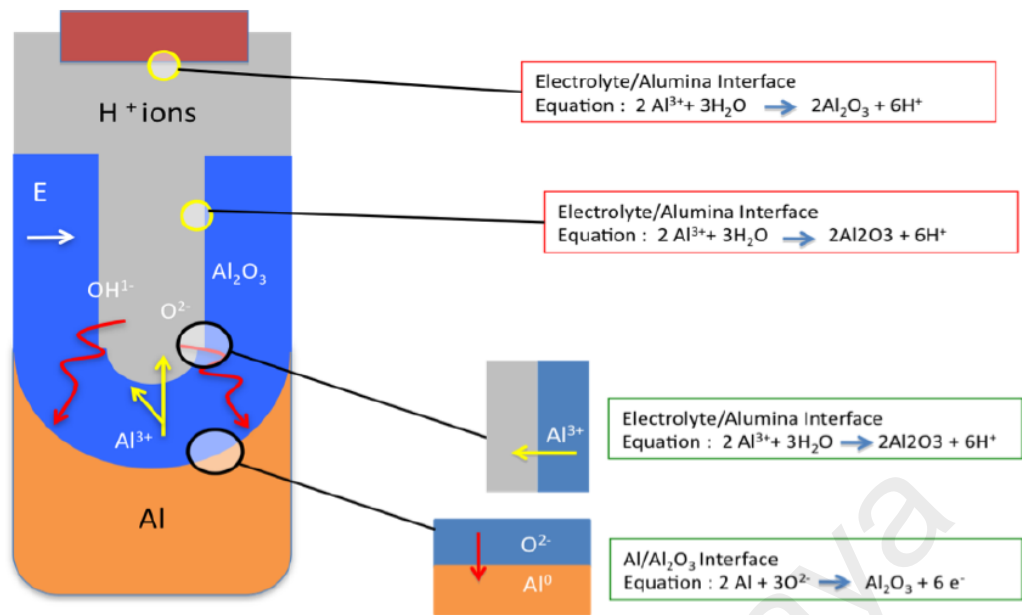


Figure 2.9: Chemical Half Reaction for Formation of Aluminium Oxide Nano-Porous (Abrahami et al., 2017)

Formation and growth of the porous coating is important in order to act as protection of aluminium surface against corrosion. Compared to the bare metal, anodized metals have better adhesion for paint primers and color stability can be well maintained. Therefore, the anodized aluminium and aluminium alloy parts have longer life spans as compared to the non-anodized parts. Protective surface oxide layer enhanced corrosion resistance of anodized aluminium (Krishna, 2015). In addition, formation of anodic oxide coating increases mechanical hardness of the surface contributes to improvement of corrosion properties. Anodizing offers many benefits in the metals industry with low initial finishing cost as well as low maintenance costs for value in long term.

Many sectors of industry are using the principal applications of anodized aluminium which as shown in Table 2.5.

Table 2.5 : Applications of anodized aluminium alloys in industrial

Industry	Applications
Building	Anodized aluminium is used as the material to produce decoration and protection of exterior components of buildings such as window frames, ceiling panels, etc.
Transportation	Landing gear, engine block, fuel pumps, brake pistons
Consumer durable goods	Shelves, cooking utensil covers, furniture, costume jewelry, giftware
Lighting	Indoor lighting fixtures, reflectors on highway
Electrical	Capacitors, insulated wire and strip insulators

2.3.1.2 Intermetallic Phases of Aluminium Alloys with Nano-porous

Intermetallic phases or particles of aluminium alloys with differ composition, dimension, shape, density and morphology can be studied by observing the microstructure of aluminium alloys. It has significant effect on the commercial aluminium alloys that are anodized. During anodizing treatment process, material behavior of the intermetallic phases has control of microstructure and final morphology of the aluminium nano-porous coating formed.

Microstructure and surface morphology of each class of aluminium alloy is differ from each other which as shown in Figure 2.10. Hence, the parameters for surface modifications are conducted in compatible with the constituents of aluminium alloys.

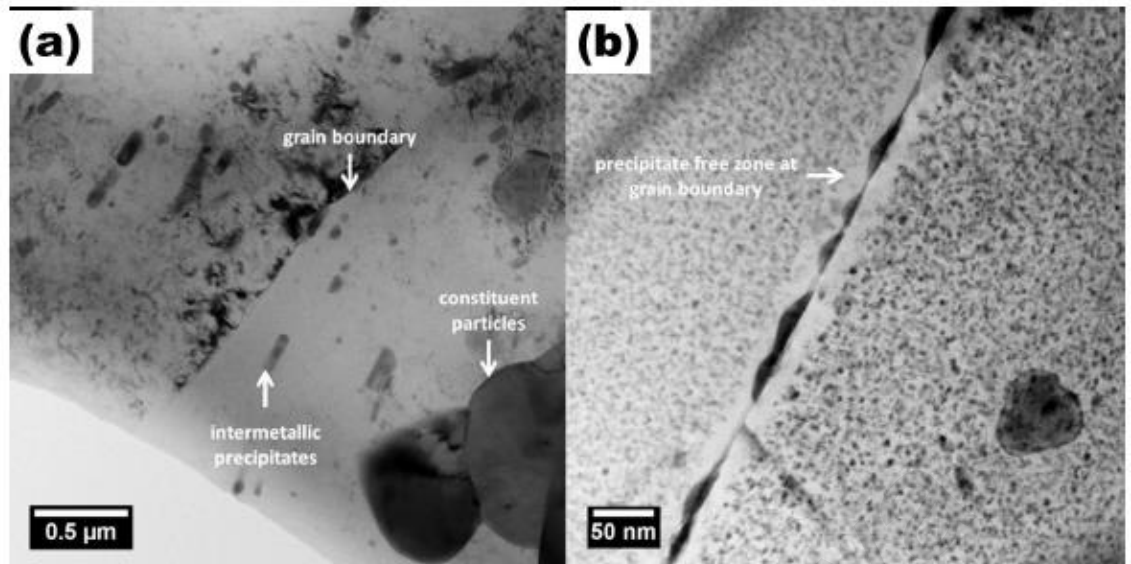


Figure 2.10: Bright field TEM micrograph showing typical microstructural variations in specimens of Al alloys: (a) AA2024-T3 and (b) AA7075-T76 (Li et al., 2015).

Aluminium oxide layer solubility is determined by the intermetallic phases' electrochemical nature. There are two possibilities of phenomenon anodizing process: the aluminium oxide might dissolve in the electrolyte or it will undergo oxidation and consolidated into the anodic layer or coating. In the case that the aluminium nano-porous coating formed on the intermetallic phases has lower formation kinetics than the aluminium substrate, the nano-porous coating has high potential to be integrated either in the state of partially oxidized or unoxidized with the anodic layer (Li et al., 2015).

It is vital to ensure good adhesion of intermetallic between aluminium substrate and the aluminium nano-porous coating formed on the surface. Various intermetallic phases that found in aluminium alloys are classified in terms of size range, morphology and constituting elements which as shown in Table 2.6.

Table 2.6: Classification of Aluminium Alloys Intermetallic Phases

Classification	Size Range	Morphology	Constituting Elements
Phases formed by precipitation, mostly from a super saturated solid solution that is subjected to low temperature ageing treatment	1 nm to 1 μm	Spherical, needle like, laths, plate like	Cu, Mg, Si, Zn and Li.
Phases formed during alloy solidification	Few tenths of a μm to 10 μm	Large and irregularly shaped	Cu, Fe, Si and Mg
Phases that are insoluble in Al and termed as dispersoids. Generally found as segregates, clusters or nodules in solutionised state and most often responsible for grain refining	0.05 μm to 0.5 μm	Nodular or irregular	Cr, Zr, Ti and Mn

In the case that oxidation rate of intermetallic phases is higher than the aluminium matrix, the intermetallic phases will be oxidized completely and there is possibility that to be incorporated with the electrolyte. Movement of particles during oxidation of the intermetallic will determine the optical appearance of the anodized aluminium alloys. Another factor that also contribute to anodized aluminium alloys' optical appearance is the type of alloying element used in anodizing treatment process.

2.3.1.3 Optical Appearance of Aluminium Alloys with Nano-porous

Interaction of light with the material, a complex phenomenon takes place in the surrounding with the presence of light resulting in the optical appearance that justifiable by human beings' naked eyes (Tilley.R, 2010). Through the interaction of light with the surface of anodized aluminium alloy, specific optical appearance is formed. Light reflects

from the two objects: anodized layer surface, interface between aluminium nano-porous layer and aluminium substrate. Thus, optical appearance of the aluminium nano-porous layer is formed through light absorption within the aluminium oxide layer and intertwine with the scattered light.

Optical surface appearance of anodized aluminum is various from one another. It can be in glossy metallic look, bright or oppositely in dark black. Despite of that, up to date, commercial anodized aluminium by decorative anodizing process unable to achieve bright, glossy and white surface. Failure to achieve white anodized aluminium is due to the application of aluminium anodizing by colour generation from anodized aluminium surface unable to be applied for white surface forming. Therefore, only via scattering of light, white surface of anodized aluminium alloy can be attained. For anodized aluminium alloy, colouring absorption technique can be adopted to suit the functionality of the end products or fulfil certain consumer products design.

2.3.1.4 Electrochemistry of Aluminium Alloy Nano-porous

In terminology of electrochemical, when a pure substrate that free from oxide is being immersed to the solution, atoms from metal surface tends to release metal ions into the solution, or known as dissolution of metal. Oxidation reaction takes place at the anode where metal corrodes. Balanced electrons caused negative charges accumulate on the metal.

Standard electrode potential is a measurement on the tendency of metal ionization in solutions for the metal or metal ion reaction which can be represented by the equations below:



At where, M represents atoms on metal surface; M^{n+} is ionized ions in solution; ne^- symbolized electrons from the metal.

$$E_{r, M^{n+}/M} = E^\circ_{M^{n+}/M} + \frac{RT}{nF} \ln a_{M^{n+}} \quad (2.12)$$

At where, E_r is reversible potential and E° is standard reversible potential; $a_{M^{n+}}$ is dissolved metal ions

Potential difference between metal and the solution is simply known as electrode potential, E_{corr} which is negative. Formation of metal ions then will be inhibited by electrode potential as the dissolution of metals is inhibited and despite of that, metal ions formed in the solutions will be deposited on the metal. Ions dissolution rate and ions deposition rate will be equaled as the process continued and stable potential is achieved, which expressed as reversible potential, E_r . E_r is highly depend on the concentration of the metal ions dissolved and standard potential of metal ions dissolved in the solution (Hinds, n.d.). Rate of corrosion is equivalent to the corrosion current density, I_{corr} (Corrscience.com, 2011). The data are tabulated in the polarization curve as shown in Figure 2.11.

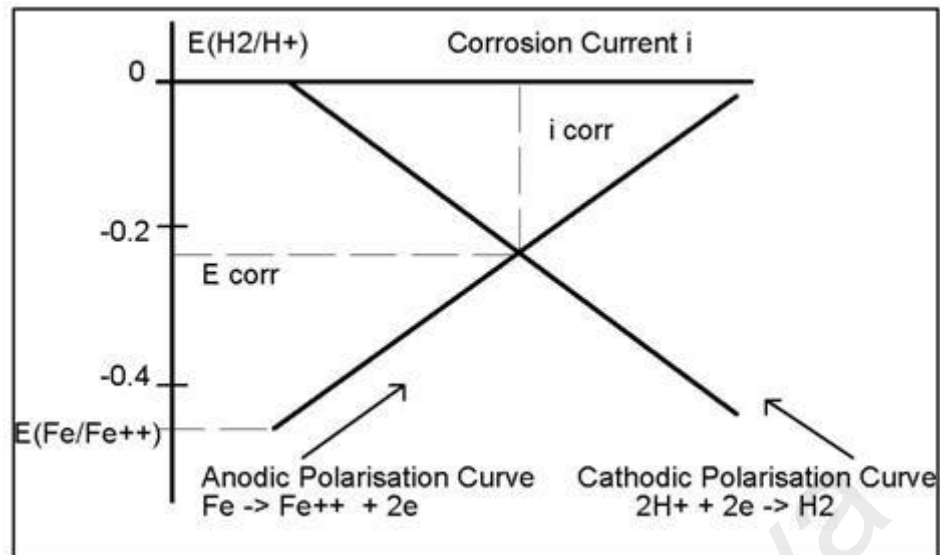


Figure 2.11: Schematic polarization curve for corroding metal, Fe (Corrscience.com, 2011)

As discussed earlier, anodizing treatment process is carried out to form aluminium nano-porous on the surface of aluminium. Parameters like thickness of layer, size and diameter of pores as well as other properties of the aluminium nano-porous formed have direct relationship with the steady-state voltage applied during the anodizing treatment process (Poinern, Ali and Fawcett, 2011).

Graph in Figure 2.12 shows the effect of current and voltage on the aluminium sample surface during anodizing treatment process. It is clearly shown that at extreme high voltage and low current, thick layer of porous oxide layer formed. On the contrary, crystal boundary attack and leads to pitting at the boundary of nano-porous crystallography at very low voltage and high current. As the current decreases whereas voltage increases, electro-polishing effects occurs. With further decrease in current, the voltage is increased, porous layer will be formed on the surface of aluminium substrate (Dehnavi, 2015).

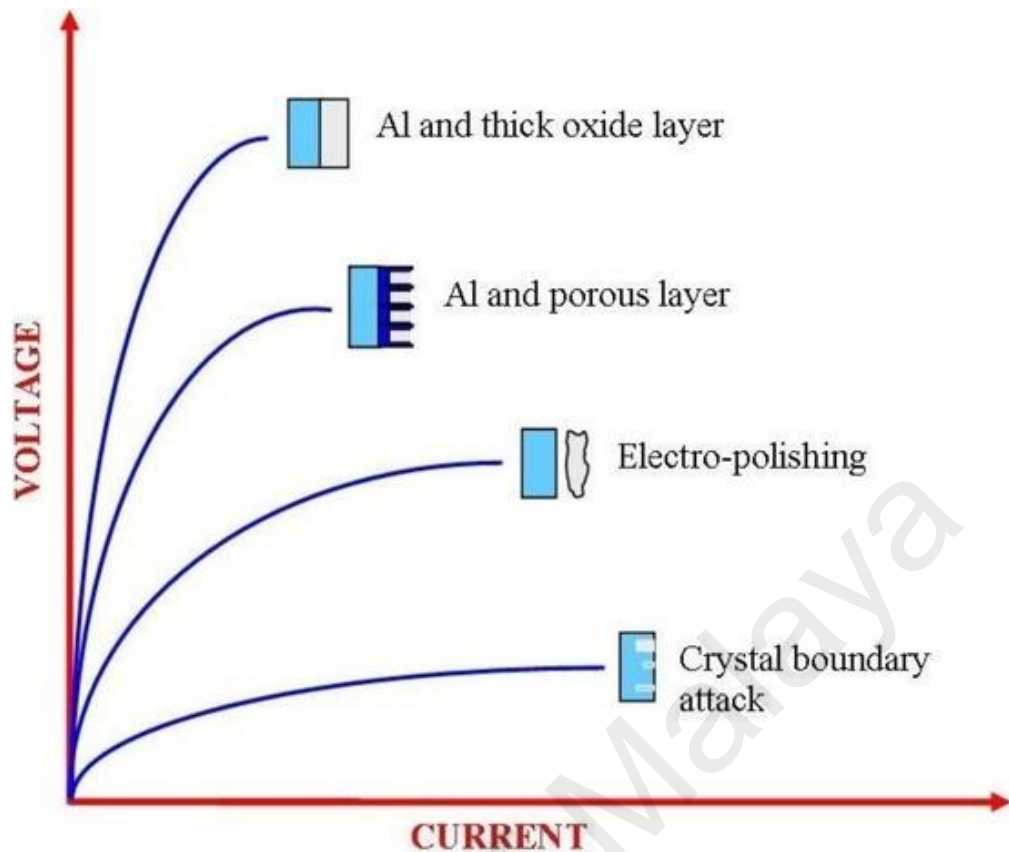


Figure 2.12: Anodic polarization of aluminum in different electrolyte solutions (Fan et al., 2015)

2.3.1.5 Adhesion of the Aluminium Nano-porous with Substrate

Composition of the oxide and feature of morphology will have impact the oxide properties. Adhesion of the coating and substrate in materials have been presented in many theories which including diffusion rate, strength of boundary layer, physical chemical interaction or adsorption and mechanical interlocking. The most relevant theories for metal or polymer bonding in aluminium alloy are adsorption and mechanical models.

According to the findings of few researchers, achievement of strong adhesion between aluminium nano-porous and the substrate is predominantly caused by mechanical interlocking (Sharma, Eden and Golesich, 2014). Adversely, there are studies find out

that oxide chemistry also dominant factor to determine the nature and interaction of oxide with organic resin (Elham Farouk, 2018) Based the study carried out, electrolyte used in the anodizing treatment process and mechanical interlocking do not have any impact on the adhesion strength. Despite of this, size of nano-porous affects the adhesion strength. The larger the pore size, the better the performance of nano-porous. In another research finding by, this statement is denied as pore with size of about 25nm do not show any improvement on the adhesive strength. Hence, the dominant mechanism of adhesion is not firmly affected by mechanical interlocking and pore size which is the contact area between anodic layer and the substrate. Strength of adhesive is possibly improved by either of the factors.

2.3.1.6 Wettability of Anodized Aluminium

Interface between nano-porous formed and substrate stability under ingress of water, which knows as the wettability is dominantly depends on the parameters of anodizing treatment process, mainly type of electrolyte used, electrolyte concentration and the temperature to carry out anodizing. In addition, wettability of anodized aluminium alloy is very much affected by the oxide chemistry effect. In the presence of hydroxyls at the surface, chemical reaction will take place in between the oxide and the resin. Surface roughness will have direct impact on the wettability of the anodized aluminium alloy and its morphology changed when chemical reaction occurs.

2.3.2 Annealing of Aluminium

Annealing is one of the heat treatment method that very commonly adopted in the industry for high end applications. Another heat treatment though is surface hardening that carried out in order to enhance the surface hardness. Thermochemical treatments are applied which also known as case hardening. It is optional to carry our quenching. Interior

structure or properties will be remained whereas the surface will be undergoing modifications.

For aluminium, it is crucial to distinguish whether the specific series of aluminium alloy is heat treatable or non-heat treatable. Cold work is applied to both wrought and cast aluminium alloys whereas heat-treatable alloys can be strengthened by precipitation hardening through heat treatment. Normally, temperate ranged from 300 to 400°C is used in aluminium annealing process (AZoM.com, 2004). However, it varies from the series of aluminium alloy. There are three physical stages to carry out precipitation hardening: solution heat treating, quenching and aging.

Annealing is different from precipitation hardening as it occurs in three steps which are recovery, recrystallization and grain growth. Effect of heat treatment temperature on hardness of the AA7075 under annealing is shown in Figure 2.12. It is clearly seen that the hardness of the AA7075 reduced when temperate of heat treatment is in between range of 260 to 310°C.

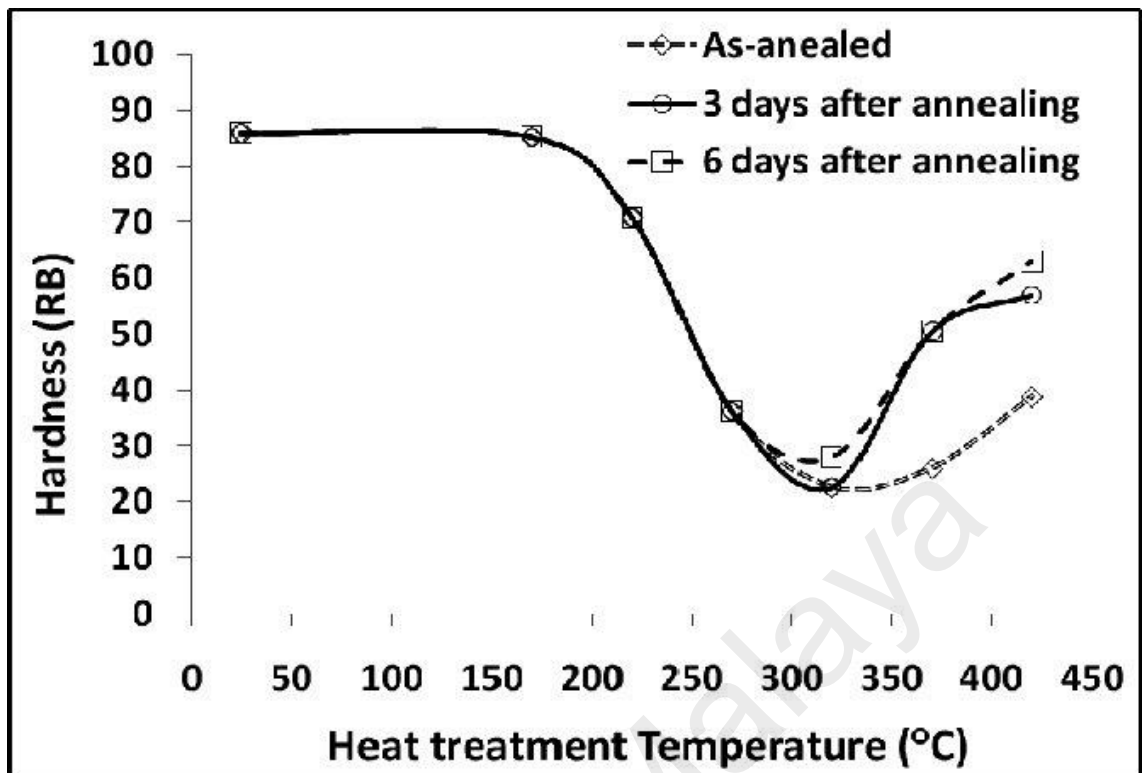


Figure 2.13: Effect of annealing temperature on hardness of 7075 aluminum alloy (Fallahi, Hosseini-Toudeshky and Ghalehbandi, 2013)

2.4 Corrosion Characterization Techniques

Corrosion of metals or alloys is destructive and occurs all the time that might cause corrosion failures which could lead to significant impairment to the function of the metal, the environment, or the technical system. Hence, corrosion characterization is conducted to evaluate and select materials that are suitable to be used in specific environment to minimize chances of corrosion to take place. Corrosion control can be achieved through corrosion characterization by taking different means of prevention. Few corrosion characterization techniques can be attained in order to venture into its corrosion mechanisms.

Primary corrosion characterization can be carried out or justified through visual inspection via naked eyes or using microscope. Visual inspection is simply adopted in order to diagnose corrosion failures as each form of corrosion has its significant causes. As mentioned in Chapter 2.2.1, Group 1 type of corrosion is able to be identified by visual inspection. The microstructures of the materials and its surface morphology can be studied through microscopic observation.

Corrosion behavior also can be investigated through corrosion testing conducted in the laboratory.

University of Malaya

CHAPTER 3: METHODOLOGY

The flow of research study is as shown in Figure 3.1.

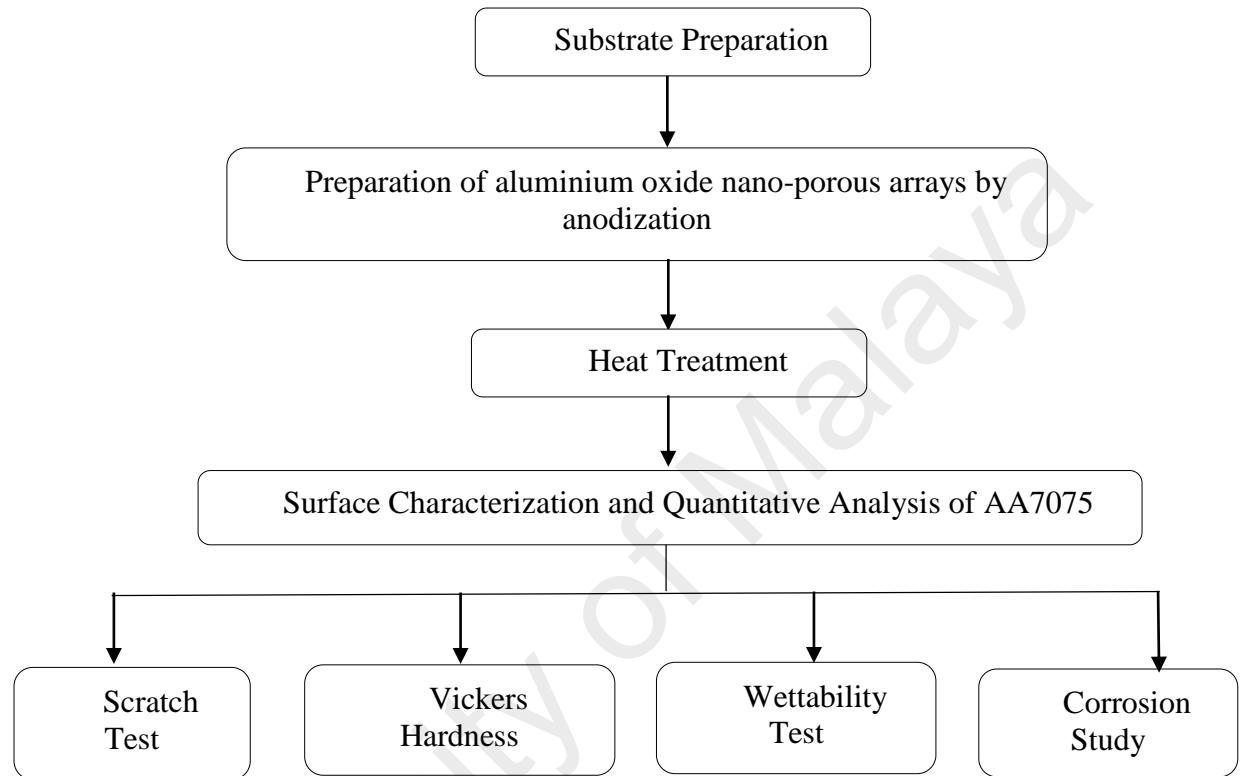


Figure 3.1: Flow of Research Study

3.1 Preparation of Samples

Substrate used in this research study is aluminium alloy series, which is AA7075-T6. It is fabricated (from KAMCO ALUMINIUM SDN BHD, Kuala Lumpur, Malaysia) in plate form and wire cut into dimensions of 15 mm × 15 mm × 2 mm as shown in the Figure 3.2 There are 20 pieces of samples are prepared for experimental purpose. Grinding of substrates are carried out by using silicon-carbide emery papers with 800–2400 grit, followed by wet-polishing using a diamond slurry. Then, the substrates were rinsed with distilled water for about three times and sonication in acetone for 10 minutes at temperature of 40 °C by using ultrasound sonicator as illustrated in Figure 3.4. Sample grinding and polishing is carried out by using the grinding machine at the laboratory as shown in the Figure 3.3., followed by drying at temperature of 100 °C for an hour to remove the water droplets. The steps are repeated for every single substrate sample before proceed for the fabrication of thin film of aluminium oxide nano-porous arrays.

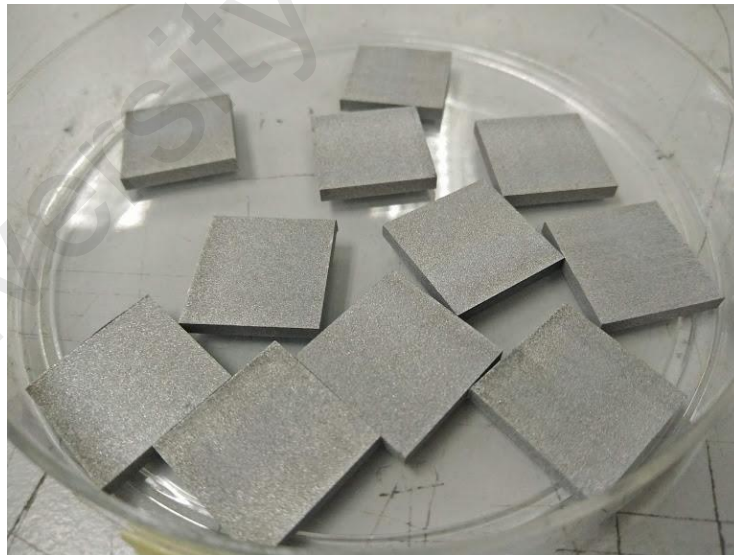


Figure 3.2: AA7075-T6 samples cut into size of 15 mm × 15 mm × 2 mm.



Figure 3.3: Grinding Machine



Figure 3.4: Ultrasound Sonicator

3.1.1 Preparation of Anodized and Heat-treated Samples

Anodizing treatment and heat treatment process have been chosen in this study for the formation of self-organized aluminium oxide nano-porous arrays in order to improve the corrosion resistance of AA7075. Anodization is carried out by application of electrochemical process. To set up the electrochemical cells, two electrodes are required and electrolyte to allow chemical reactions of anodic and cathodic reaction to take place.

Set up of the experiment is illustrated in Figure 3.5. Direct current (DC) of 12 V is used as power source (Model E3641A, Agilent Technologies, Palo Alto, USA) in the anodizing treatment process for duration of 1 hour, which as shown in Figure 3.6. Electrochemical anodization is carried out by preparing two electrodes, at where graphite rod is selected as cathode and sample acts as anode. Graphite rod has diameter of 7mm and the sample is clamped at the anode (Figure 3.7). Anode and cathode are kept at distance of 20mm for the anodization of all the samples. Electrolyte used in the electrochemical cell is 15 wt% H₂SO₄. Samples were rinsed with de-ionized water or distilled water after anodization in order to remove contaminants or residual substances on the sample surface. Avoid direct touching of the anodized sample surface by holding the sample edge. After cleaning, the anodized samples were proceeded with heat treatment process. Crystalline phases will be formed by heat treated the samples with temperature of 450°C for duration of 1.5 hour. Annealing is conducted surrounding condition by applying heating and cooling rate of 5 °C/min..



Figure 3.4: Experimental equipment to carry out anodization treatment process for producing aluminium oxide nano-porous arrays

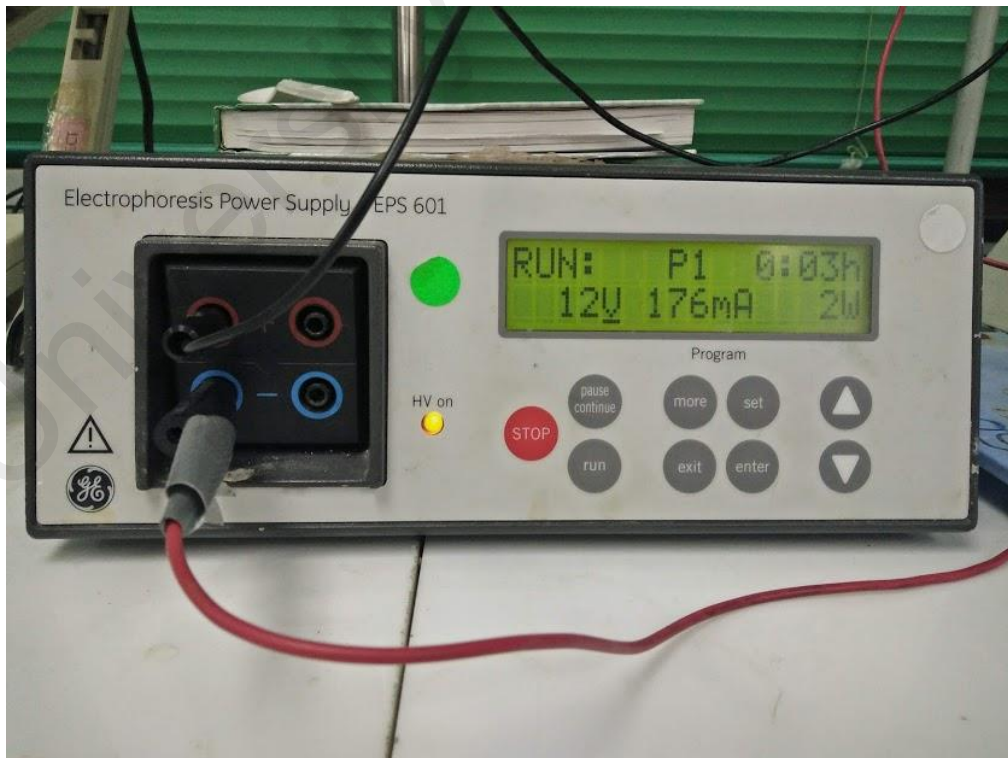


Figure 3.5: Power source of direct current (12V) used in the experiment

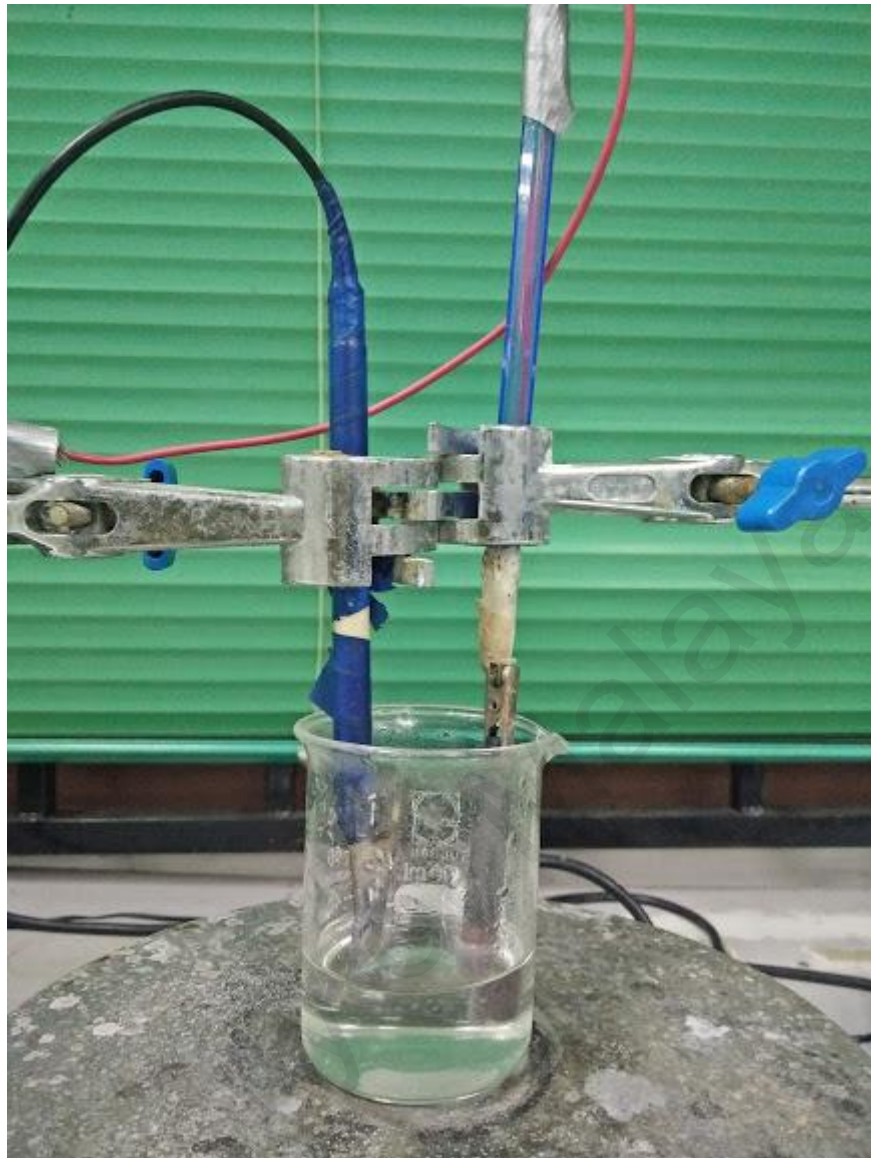


Figure 3.6: Set up of electrodes for electrochemical process

3.2 Surface Characterization

Phase analysis and microstructural characterization are applied for aluminium alloys surface characterization study. The morphology of coatings was investigated using a field emission scanning electron microscope (FESEM, SU8000, Hitachi, Japan) with an acceleration voltage of 1 to 2 kV. The cross-sections of the specimens were prepared with a destructive technique using a high-precision cutter equipped with a diamond blade. The

phase composition and purity of the substrates, Al₂O₃ Nano-porous arrays heat treated Al₂O₃ Nano-porous arrays on series 7 specimens were analyzed by X-ray diffractometry (XRD; Philips PW1840, the Netherlands) with Cu K α radiation ($\lambda=1.54178 \text{ \AA}$) functioning at 45 kV and 30 mA, 2 theta range of 30°-80°, scan rate of 0.1°·s⁻¹, and step size of 0.026°. The "PANalytical X'Pert HighScore" software was also employed to check the XRD patterns, wherein all the reflections were equated with the standards gathered by the Joint Committee on Powder Diffraction and Standards (JCPDS, card #005-0682). The atomic concentration as well as the two-dimensional distribution of the constitutive elements were respectively determined using energy dispersive X-ray spectrometry (EDS) (Sarraf, 2018).

3.3 Quantitative Analysis on Samples

3.3.1 Adhesion Strength

The adhesion strength of the coatings was measured quantitatively using a Micro Materials Nano Test (Wrexham U.K) equipped with a diamond indenter with radius and angle of $25.0 \pm 2.0 \text{ }\mu\text{m}$ and $90.0 \pm 5.0^\circ$, respectively. The experiments were performed with a velocity of 5 mm s^{-1} and the loading rate gradually increased to 9.2 mN s^{-1} . The scratch tests were repeatedly performed on each sample and the damage profile was investigated under a light optical microscope (Olympus BX61, Tokyo, Japan). Here, the adhesion strength is defined as total coating failure. The sample was moved perpendicular to the scratch probe whilst the contact was either held constant or ramped at a user-defined rate. Throughout the test the probe penetration depth and frictional load were continuously monitored. A pre-scratch scan was accomplished using an ultra-low contact force in order to assess baseline sample topography. After that, the scratch test was repeated three times within the specified load range using a diamond indenter.

For further investigation, the scratch hardness test was performed on the Al₂O₃ Nano-porous arrays, heat treated Al₂O₃ Nano-porous arrays thin films at 450°C for 1.5 h. This test was executed to measure the resistance of the thin films to permanent deformation under the action of a single point (stylus tip) and involves a different combination of properties of the surface because the indenter, in this case, a diamond stylus, moved tangentially along the surface. The scratch hardness test, is more appropriate technique to measure the damage resistance of a material, like the two-body abrasion (Sarraf, 2018). This technique is applicable to a wide range of materials including metals, alloys and some polymers. This test is based on the measurement of the residual scratch width, after the stylus is removed to compute the scratch hardness number. Therefore, it reflects the permanent deformation resulting from the scratch and not the instantaneous state of combined elastic and plastic deformation of the surface. Since the state of stress at the stylus tip is a function of contact geometry and applied force, the magnitude of the scratch hardness number is dependent upon both the stylus tip radius and the normal load. The scratch hardness number is calculated by dividing the applied normal force on the stylus by the projected area of the scratch contact, assuming that the hemispherically-tipped stylus produces a groove whose leading surface has a radius of curvature r , the tip radius of the stylus. The projected area of the contact surface is therefore a semi-circle, whose diameter is the final scratch width. The critical load is defined at the onset of the coating loss, which is associated with the appearance of the metallic substrate inside the scratch channel. This measurement was accomplished with the help of an optical microscope. The tester was also enabled to obtain the frictional coefficient at the critical load (Ruckh et al., 2008, ASTM, 2003, Jaworski et al., 2008). The scratch hardness, HS_p was estimated following the specification of ASTM G171-03 norm:

$$HS_p = \frac{8P}{\pi w^2} \quad \text{Eq. (3.1)}$$

Where HS_p , P and w are the scratch hardness number, normal force and the scratch width, respectively.

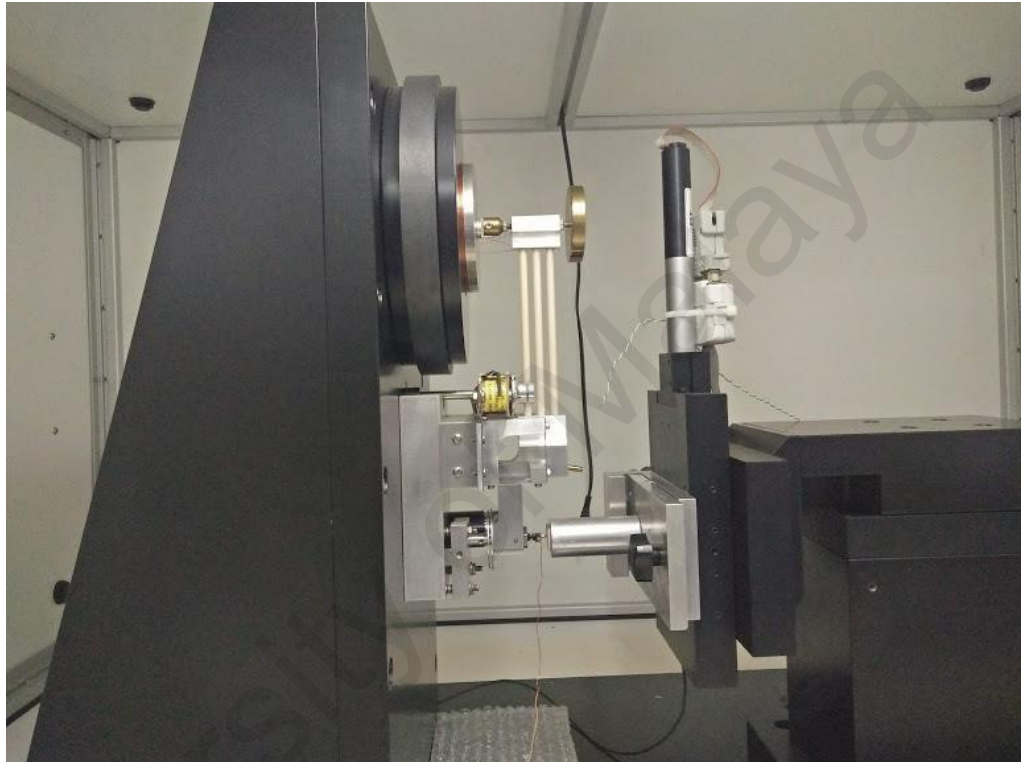


Figure 3.7: Machine used to conduct scratch test

3.3.2 Microhardness

The microhardness of the samples was quantified using a Vickers microhardness testing machine (Mitutoyo-AVK C200-Akashi Corporation, Kanagawa, Japan) which as shown in Figure 3.8. The test is conducted by the indentation-strength method at room temperature using an applied load of 98.07 mN and a dwell time of 15 s. Five indentations per sample were done to determine the average value of the mechanical properties.



Figure 3.8: Vickers microhardness testing machine

3.3.3 Surface Wettability

The surface wettability (hydrophilicity) of the specimens was examined by measuring the contact angles of sessile drops of deionized water deposited on each specimen surface. A video-based optical contact angle measuring system (OCA 15EC, Data Physics Instruments GmbH, Germany) was utilized to inspect the optical wettability. A constant liquid volume of 5 μl was used for the contact angle evaluations of all the specimens using a drop velocity of 2 $\mu\text{l s}^{-1}$ at a temperature of 26 ± 1 °C. The droplet height

“*h*” and width “*d*” were measured to calculate the contact angle “ θ ” as follows (Elias et al., 2008):

$$\theta(^{\circ}) = 2 \tan^{-1} \left(\frac{2h}{d} \right) \quad \text{Eq. (3.2)}$$

3.4 Corrosion Studies

Potentiodynamic polarization measurements were carried out in a single compartment cell using a standard three-electrode configuration: a sample as the working electrode, saturated calomel electrode (SCE) as a reference and a platinum electrode as counter electrode. The surface area exposed to the test solution was 1cm². All the experiments were performed in artificial seawater. A potentiostat Bio-Logic SP-150 monitored by a PC computer and EC-Lab software were used to collect and evaluate the experimental data. Potentiodynamic polarization curves were recorded in the potential range –2000 to +2000mV versus SCE reference electrode at a scan rate of 1mVs⁻¹, after allowing a steady-state potential to develop. Duplicate tests were performed under identical testing conditions to verify reproducibility.

3.4.1 Preparation of Artificial Seawater

The electrolyte corrosion study was artificial seawater in the room temperature. According to the Burkholder’s formulation B, the compositions of the simulated seawater were as follows (per litre): 23.476 g NaCl + 3.917 g Na₂SO₄ + 0.192 g NaHCO₃ + 0.664 g KCl + 0.096 g KBr + 10.61 g MgCl₂·6H₂O + 1.469 g CaCl₂·6H₂O + 0.026 g H₃BO₃ + 0.04 g SrCl₂·6H₂O + 0.41 g MgSO₄·7H₂O + 0.1 g NH₄Cl + 0.1 g CaSO₄ + 0.05 g K₂HPO₄ + 0.5 g tri-sodium citrate + 3.5 g sodium lactate + 1 g yeast extract. The pH was adjusted to 7.5 ± 0.1 using a 5 M NaOH solution (Yuan et al., 2013).

3.4.2 Electrochemical Polarization

The corrosion current (I_{corr} / $\mu\text{A cm}^{-2}$), corrosion potentials (E_{corr} / V_{SCE}) and polarization resistance (R_p / $\Omega \text{ cm}^{-2}$) were achieved from the Tafel plots. The corrosion protection efficiency ($P.E.$) was also estimated using the following equation (Yu et al., 2014):

$$P.E.(\%) = \frac{I_{corr}^0 - I_{corr}^c}{I_{corr}^0} \times 100 \quad \text{Eq. (3.3)}$$

Where I_{Corr}^0 is the corrosion current of the bare series 7 and I_{Corr}^c is the corrosion current of the coated sample.

CR was calculated by the following formula:

$$CR(\text{mmyear}^{-1}) = \frac{0.13I_{corr}(E.W.)}{d} \quad \text{Eq.(3.4)}$$

where $E.W.$, d , and I_{corr} are equivalent weight of the corroding species in g, density of the corroding species in g cm^{-3} , and corrosion current in A cm^{-2} .

CHAPTER 4: RESULTS AND DISCUSSIONS

4.1 Surface Characterization

Anodization treatment process enables generation of oxide layer on the aluminium alloy series 7075 sample surfaces. When the power supply is activated, an uneven layer of oxide layer which is white in colour slowly deposited on the surface of substrate. It can be observed though naked eyes. Figure 4.1 shows the appearance of the anodized aluminium alloy sample after anodization.



Figure 4.1: Anodized surface of AA7075 sample

During anodization treatment process, aluminium substrate undergoes oxidation process by losing electrons which involves dissolution of aluminium. Oxides migrate to the substrate while aluminium ions move towards the H_2SO_4 and oxide interface. Ionized aluminium ions then react with the oxide ions from sulphuric acid, H_2SO_4 and form aluminium oxide, Al_2O_3 . An assumption can be made on the pores formation that only thin walls are formed. The schematic diagram of anodization is shown in the Figure 4.2.

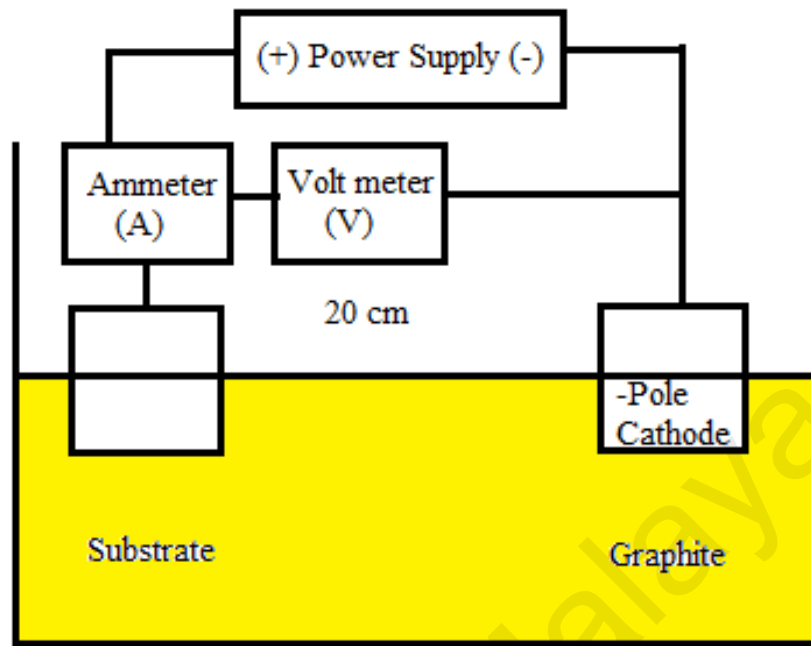


Figure 4.2: Schematic diagram of anodization treatment process

4.1.1 XRD Analysis

XRD analysis is adopted to examine the constitution of crystalline present in the composites for crystallography study (Cullity, 1956). XRD profile of substrate, the anodized sample and the heat treated sample at 450 °C for 1.5 h is shown in the Figure 4.3. From the profile obtained, XRD reflection of substrate illustrates the Al peaks at $2\theta = 38.2^\circ, 44.5^\circ$ and 64.9° , which are associated to the plane of (1 1 1), (2 0 0) and (2 2 0) respectively. Two diffraction peaks corresponding to plane of (1 1 1) and (2 0 0) can be observed as in Figure 4.3, for anodized and heat treated sample at 2θ values of 38.2° and 44.5° respectively (Al: JCPDS#004-0787). Prior to the anodization process, pre-existing oxide layer formed on the substrate surface that is commonly formed due to ambient oxygen in the atmosphere.

Trend in the peaks of XRD profile confirms the presence of aluminium oxide formation on the substrate surface.

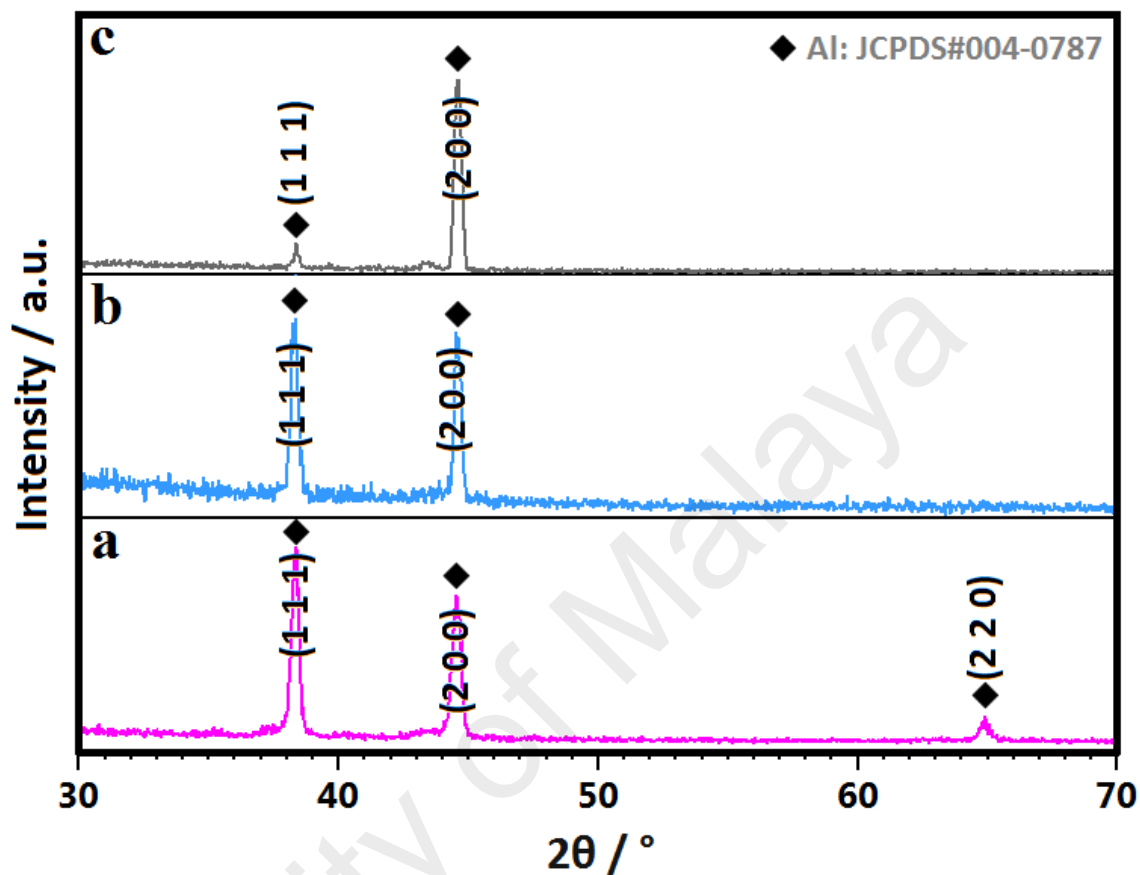


Figure 4.3: XRD profiles of the (a) substrate, (b) the anodized sample, and (c) the heat treated sample at 450 °C for 1.5 h.

4.1.2 FESEM and EDX Analysis

Surface morphology plays important role in corrosion behavior of aluminium. Characterization of aluminium oxide nano-porous arrays after anodization and heat treatment microstructure is achieved through microscopy observation which is a basic step in characterization. Morphology of substrate supports the proposition that substrate has a smooth surface with some precipitations found on it as shown in Figure 4.4.

Two FESEM images of aluminium oxide nano-porous arrays that undergo anodization for one hour at direct voltage of 12V in 15wt% sulphuric acid electrolyte are recorded: cross-section and top view. Figure 4.5 shows the top view image of anodized sample that produced by FESEM formation of pore on surface is not evenly distributed. From the cross-section view, clearly seen that nano-porous arrays formed on the surface is not in regular dimension. During anodization process, surface defects are favored sites for pore nucleation.

As per literature review on anodization, formation of irregular pits at the early stage is due to the oxide layer dissolution. Distribution of pores with larger dimension in uniform pattern can be formed with longer duration of anodization as order of pores is resulted from local perturbations (Crawford et al., 2007). Studies also revealed that presence of the alloying elements in substrate tend to reduce growth rate of oxide layer formed, which influence oxide layer structure during anodization process.

As shown in Figure 4.6, the EDS is used to study the constitutions presence in the anodized samples. Spectrum clearly shows the presence of aluminium, oxygen and minor amount of Silicon after anodization process. Two main peaks in the graph indicates the most intense surfactant concentration which are aluminium and oxide. Quantitative analysis is justified and two major elements were determined at which weightage for aluminium is 55.36% and oxygen has weightage of 40.55%. Anodic behavior of anodized AA7075 in sulphuric acid is studied and confirmed on formation of anodic oxide films above the intermetallic compounds. This anodizing characteristic influences the appearance of anodized products and most significantly increase the corrosion resistance.

However, silicon is found in the oxide layer formed in very minor content which is 4.08%. Growth of the aluminium oxidized layer can be inhibited by the network of silicon precipitates. Hence, the coating thickness formed will be reduced and leads to poor

adhesion strength. Poor adhesion strength of oxide layer formed with its substrate unable to play its role to protect the material from corrosion. Moreover, silicon which is static element will form silicon composes particles trapped inside the oxide layer. Localized dissolution around intermetallic particles as well as precipitates tends to take place during anodization, consequently pitting will occur (Shih, Lee and Jhou, 2014).

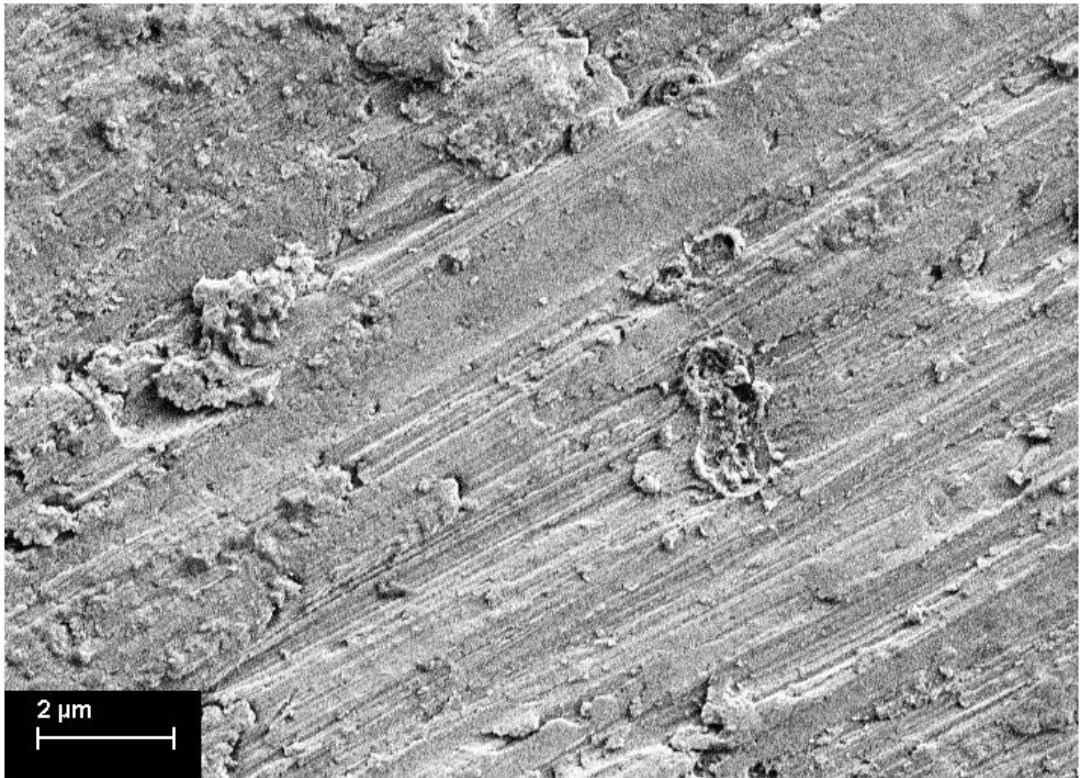


Figure 4.4: Top view FESEM images of series 7 as a substrate

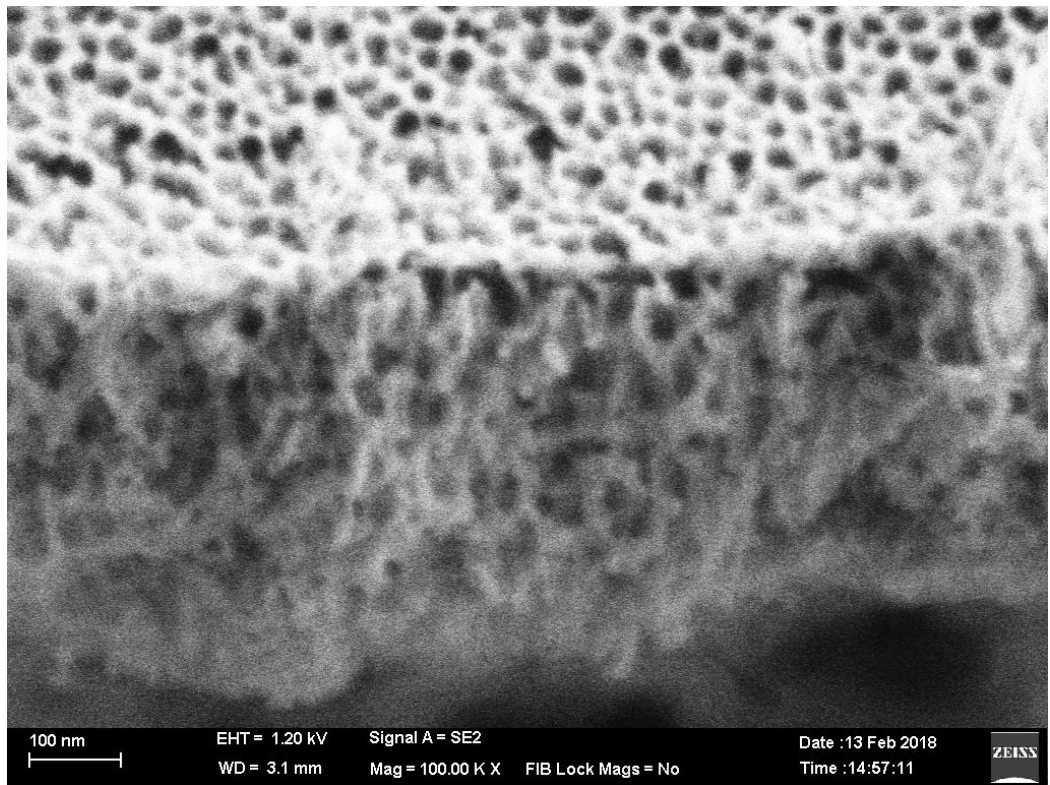


Figure 4.5: FESEM cross-section images of Al₂O₃ Nano-porous Arrays anodized for 1 h at 12 V in an electrolyte containing 15 wt% H₂SO₄.

University of

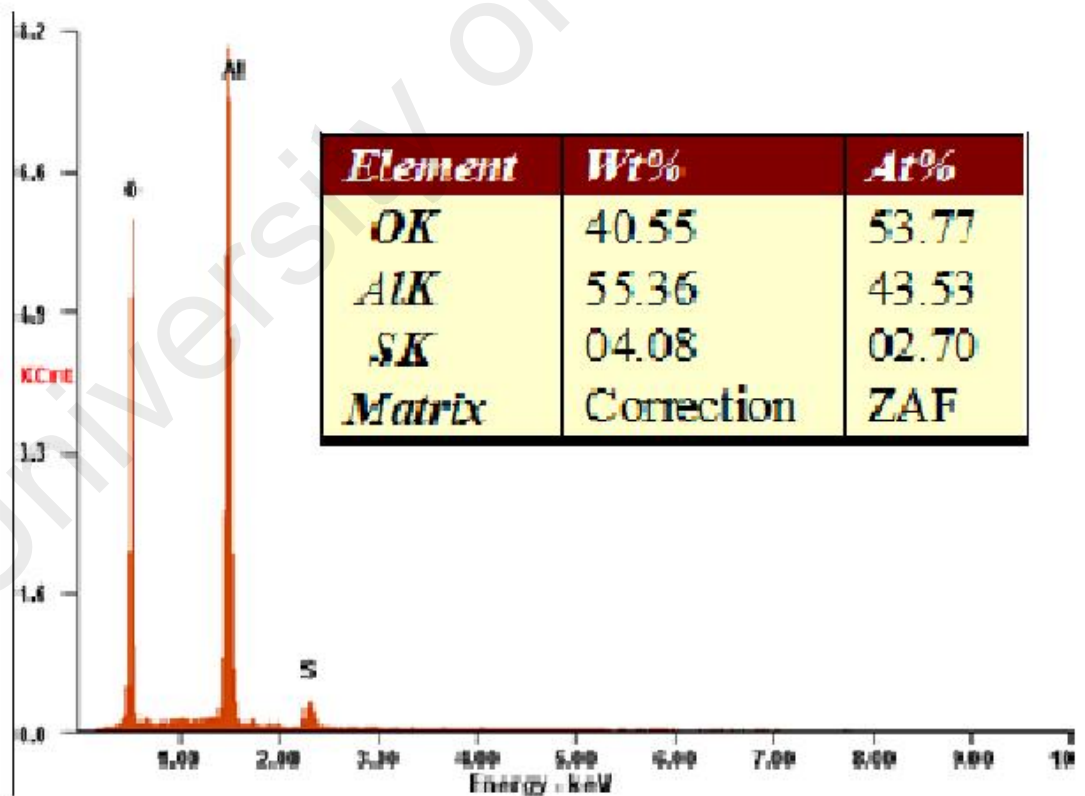
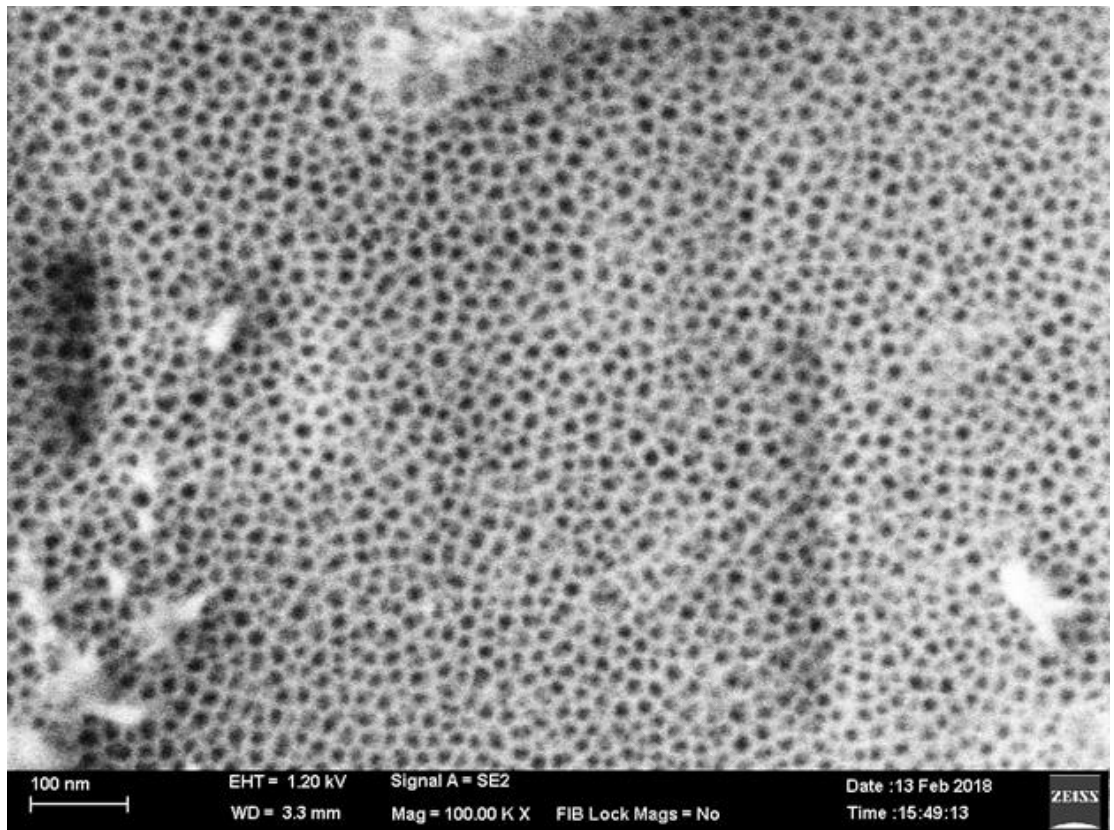


Figure 4.6: Top view FESEM images and (b) EDX of Al₂O₃ Nano-porous Arrays after anodization

4.2 Characterizations of Aluminium Oxide Nano-porous Films

4.2.1 Scratch Testing

Adhesion strength of interface between aluminium oxide film formed on the surface and substrate is studied by conducting scratch test. From the data obtained, analysis is carried out based on the three variables: depth, load and friction as. The Coefficient of Friction (COF) versus distance for the sample anodized for 1 hour in sulphuric acid. Depth of the coating indicates the thickness of the aluminium oxide film formed while load represents the adhesion strength of the layer with the substrate surface and COF refers to the friction or load.

Sliding pass is perpendicular to the aluminium oxide film. Surface damage of the sample can be seen through the image illustrated through observation using optical microscopy. Measurement for the distance of scratched surface can be done on the images formed from optical microscopy. Alternatively, SEM also can be used to perform same function. The data of the scratch test is tabulated in the graph as shown in Figure 4.7 and Figure 4.8. Based on the data collected from performing scratch test on anodized sample and heat-treated sample, the anodized sample has smaller value of failure point measured in terms of depth, load and friction. However, anodized sample has higher COF which is 0.75 compared to heat-treated sample. Abrasion or fretting resulted from high COF will cause material surface to wear and degrade, eventually corrode. This can be explained by the case-hardening of the sample surface that significantly increase the hardness of the outer surface.

Failure point indicates delamination from the oxide coating. Anodized sample show lower load in value of approximately 1733mN compared to the heat-treated sample which has critical load value of 2400mN. Scratch hardness of AA7075 at the failure point is 86 GPa after undergo anodization treatment process while the scratch hardness after heat

treatment is 93 GPa. Heat treated sample gives better adhesion strength in scratch adhesion test as it has better surface hardness than the anodized surface. From the result obtained in EDX, there is silicon precipitates on the surface of oxide film that do not form oxide layer through anodization. Hence, the observation made can justify that there is possibility the silicon precipitates lead to discontinuities in aluminium oxide layer (Hanke et al., 2013). Thus, the anodized sample surface is not well coated and has lower adhesive strength.

Adhesion strength of oxide layer on the substrate might be affected by other causes such as grain size, hardness and compatibility of substrate with the coatings. Meanwhile, the pore diameter also will give impact on the adhesion strength which also affect the wear behavior of the sample (Hanke et al., 2013). This finding is supported by the studies carried out by researchers through nanoindentation (Ng et al., 2009; Ng et al., 2011). In addition, mechanical strength of the formed coatings also give impact on the adhesion strength between layers formed and the substrate. Good adhesion strength is crucial in order for the coatings to protect the surface of materials and improve the resistance of corrosion. Hence, it can be concluded that the heat treated sample exhibits better adhesion strength compared to anodized sample.

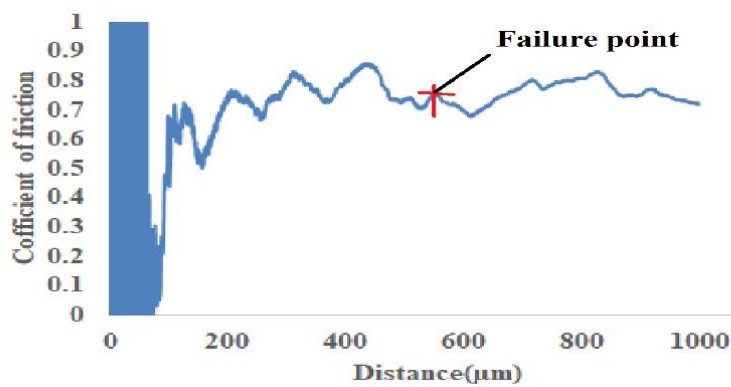
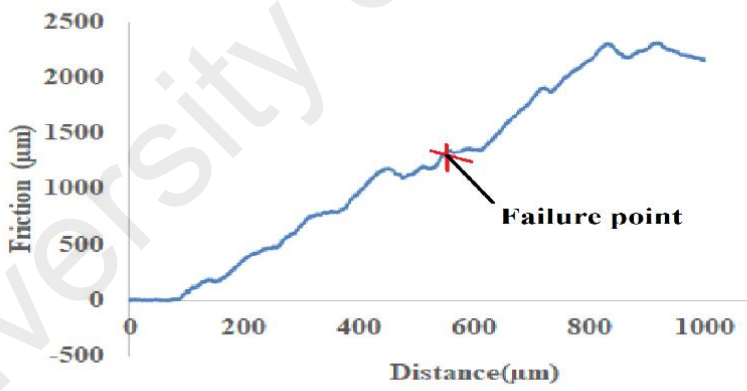
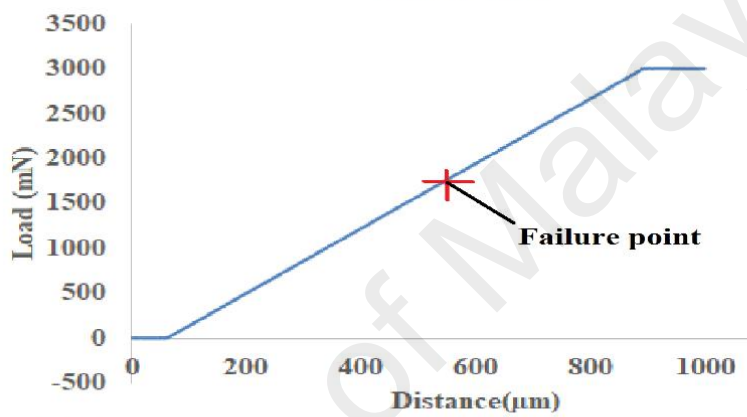
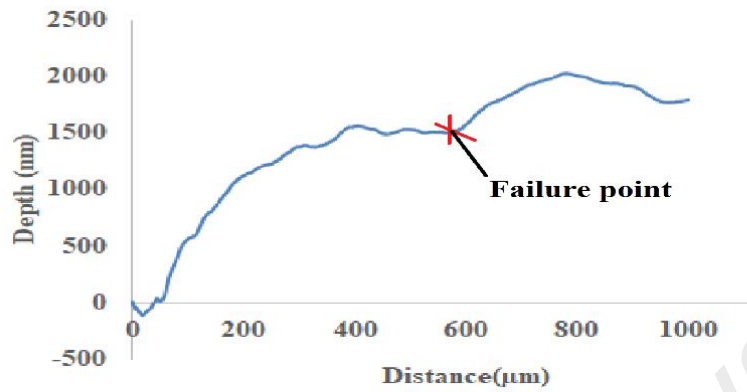
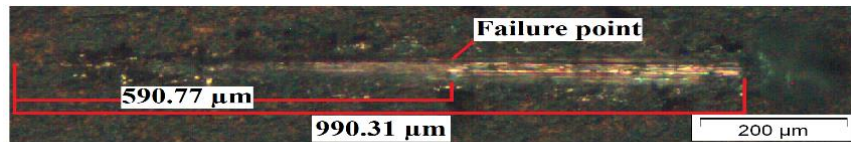


Figure 4.7: (a) The optical micrograph of scratch track and profiles of (b) depth, (c) load, (d) friction and (e) COF against scan distance after anodization.

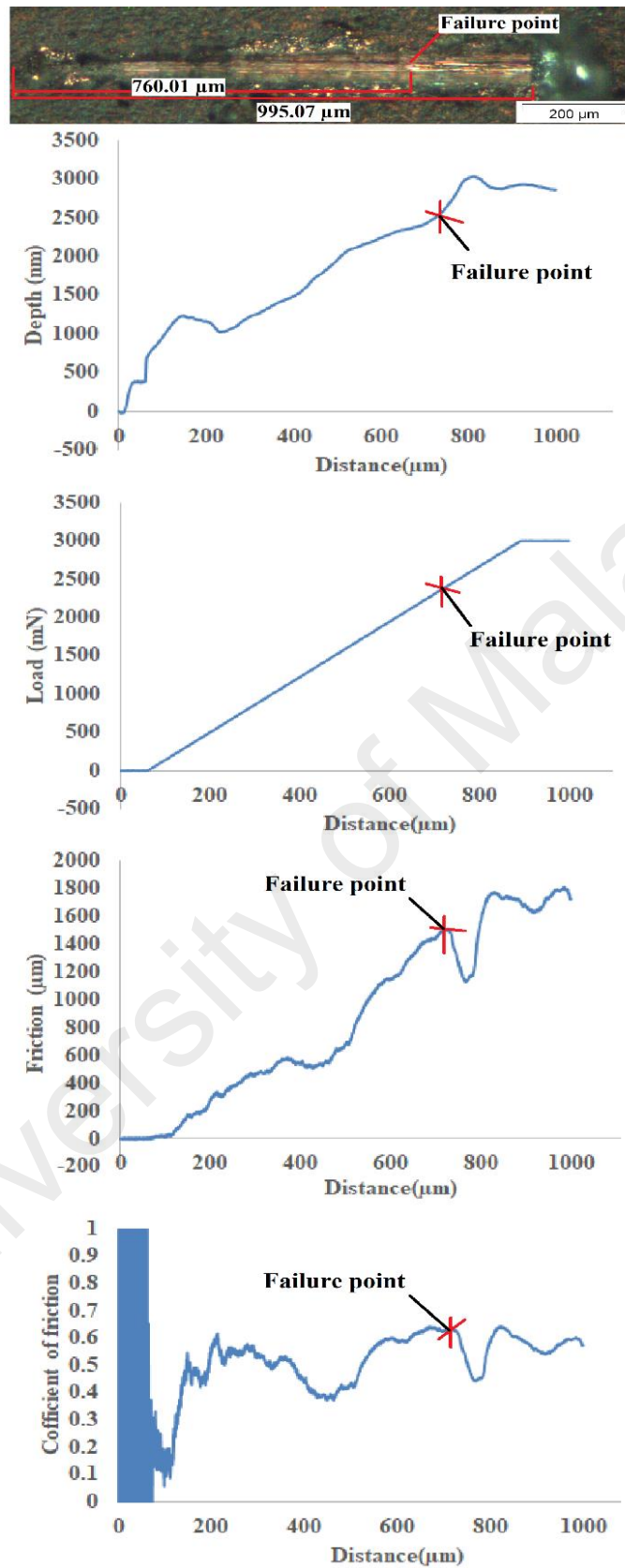
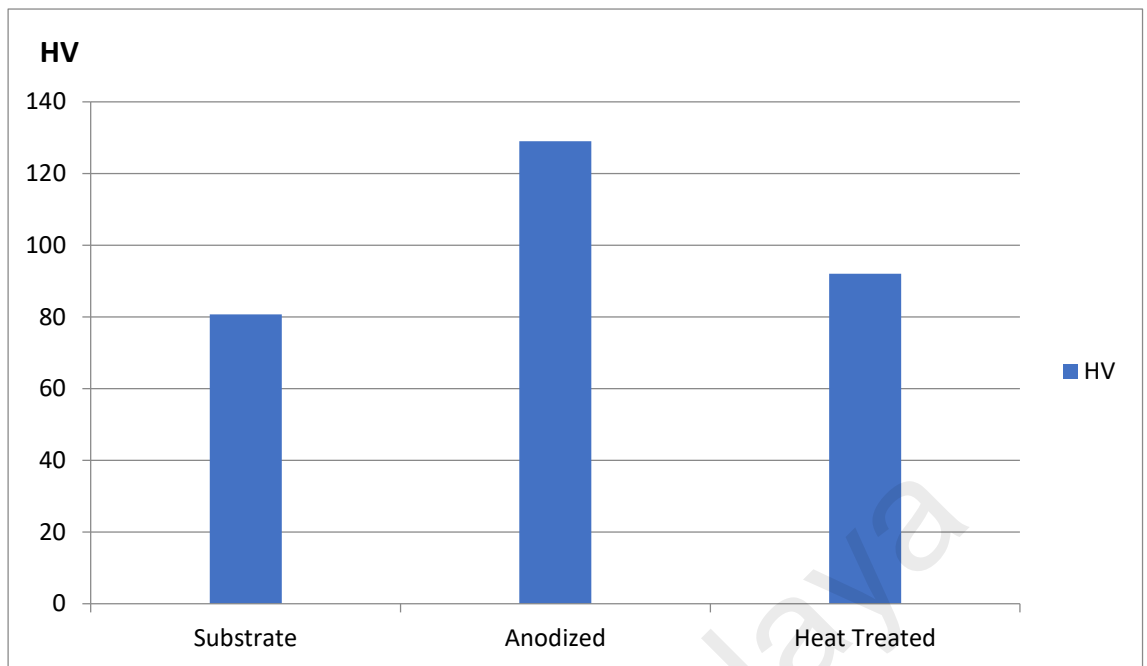


Figure 4.8: (a) optical micrograph of scratch track and graphs of (b) depth, (c) load, (d) friction, and (e) COF versus distance for the anodized sample after thermal treatment at 450 °C.

4.2.2 Vickers Hardness Test

Vickers microhardness measurement is used in evaluation of structure homogeneity and effects of surface modifications on the surface hardness of certain materials. In this study, it is carried out to study the surface hardness of AA7075 before and after surface treatment: anodization and annealing. Generally, annealing is aimed mainly to increase aluminium ductility at where sample is heated at 450°C for 1.5h and then air cooled. As indicated in Figure 4.9, anodized sample has the highest value of Disparity of Vickers Harness, followed by heat treated sample and substrate. Microhardness of substrate and heat treated samples is 80.7 and 92HV respectively, whereas anodized sample has microhardness of 129HV.

Refer to the literature review, there are stages for aluminium annealing to take place. Justification on the growth of grain size can be made during the grain growth stage. As in recrystallization stage, impingement of new unstrained nuclei formed and grow till it results in formation of new recrystallized grain structure. When the recrystallized structure is being heated for either long duration or higher temperature, there will be grain growth that will affect the mechanical properties of aluminium alloy AA7075. There are dissimilarities in other aluminium alloy at where effect of artificial aging is applied. In this study, aluminium alloy series 7075-T6 is both solution heat treated and artificially aged. Heat treatment gives big impact on the morphology of precipitates and intermetallic compounds. The growth in grain size will reduce the hardness of the heat treated sample. Hence, the heat treated sample has lower Vickers Hardness compared to the anodized sample and the substrate.



Type of Sample	Substrate	Anodized	Heat treated
Vickers Hardness	80.7	129	92

Figure 4.9: The variation of Vickers hardness value of substrate, anodized in sulphuric acid and heat treated sample at 450°C.

4.2.3 Electrochemical Polarization

Rate of corrosion reactions is influenced by the potential difference between metal and solution as it involves electrons and ions transfer between the them. Corrosion behavior of aluminium alloy also studied through analysis of potentiodynamic polarization. Polarization curves as shown in the Figure 4.10 represents the relationship between potential and current. As the potential of metal (potential difference between metal and solution) becomes more positive in its value, cathodic rate of reaction will decrease. In contrast, the rate of anodic reactions will increase, at where the metal dissolution takes

place. Polarization potential is inversely proportional to corrosion current density which represents the corrosion rate.

Polarization plots for aluminium alloy 7075 substrate, anodized and 450 °C heat treated samples are as shown in Figure 4.10. Other information obtained from polarization is recorded in Table 4.10: Corrosion potential (E_{corr}), corrosion current density (I_{corr}), corrosion rate and effectiveness of corrosion protection (P.E.) values.

Aluminium substrate has highest value of corrosion current density which equal to 1.762×10^{-5} A and corrosion potential of -0.771V. In contrast with substrate, annealing has lowest corrosion current density of 2.298×10^{-6} A. Its corrosion potential is -0.833V, which is the smallest compared to substrate and anodized samples. There is signification reduction of corrosion current density and corrosion potential after annealing, more negative readings indicate that corrosion takes place. Corrosion current density of aluminium alloy decreases by 1.05×10^{-5} after anodized, which is from 1.762×10^{-5} A to 7.163×10^{-6} A. Based on the previous study, potential is ennobled with formed oxide films in aluminium and chromium, however they broke down partially by chloride ions (in corrosion surrounding) result in localized corrosion (Hinds, n.d.).

Despite of this, the anodized sample exhibits lowest corrosion rate of 1.29×10^{-6} after heat treated, follow by the anodized sample without annealing and substrate has highest corrosion rate of 4.5×10^{-6} . From the data collected, justification can be made on anodizing and annealing that these surface modifications are able to reduce corrosion in aluminium alloy series 7075. Corrosion protection for three cases were ventured and obviously corrosion resistant is enhanced by annealing. Anodized sample after annealing treatment has the greatest percentage of protection efficiency of 78.64%, followed by anodized sample (33.44%). From the findings of data collected in the experimental of

electrochemical polarization, conclusion can be made on aluminium alloy series 7075 able to have better corrosion resistance through anodization and heat treatment process.

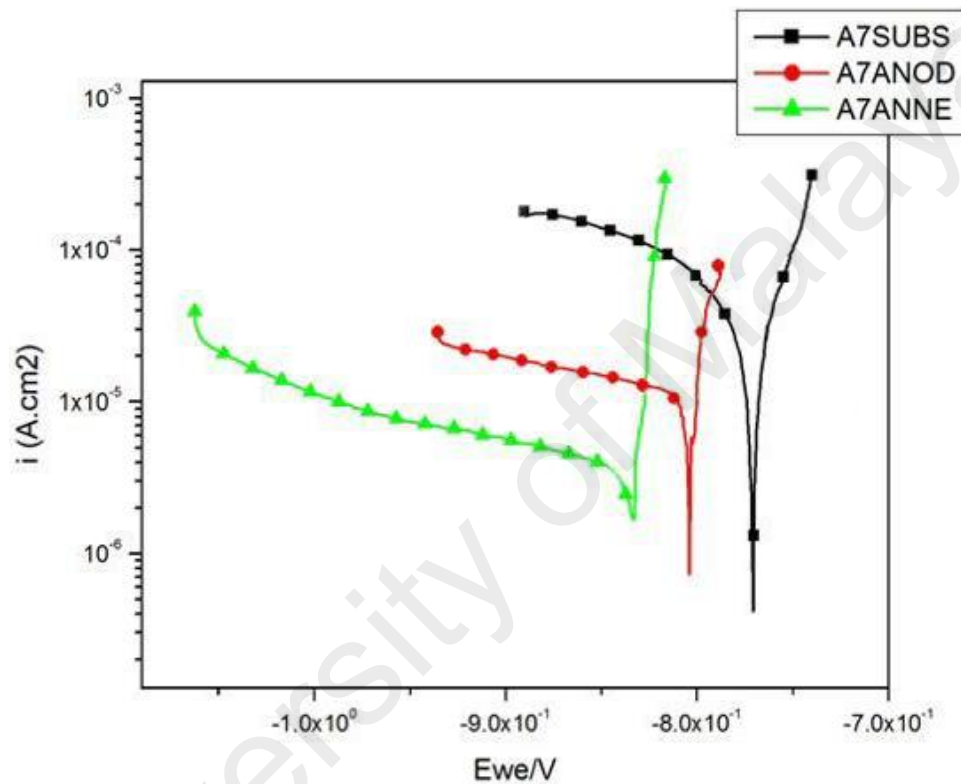


Figure 4.10: Polarization plots of the bare substrate, the aluminium oxide as-anodized specimen, and the 450 °C heat treated sample

Table 4.1: Corrosion potential (E_{corr}), corrosion current density (I_{corr}), corrosion rate and effectiveness of corrosion protection ($P.E.$) values.

Al Series 7	Substrate	Anodized	Annealing
E_{corr} / V	-0.771	-0.735	-0.833
I_{corr} / A	1.762×10^{-5}	7.163×10^{-6}	2.298×10^{-6}
$\log (I_{corr} /A)$			
Weight of samples(gr)	1.2	1.3	1.3
Density(gr/cm^3)	2.8	3.95	3.95
E.W(g)	9	17	17
Corrosion rate	4.50×10^{-6}	4×10^{-6}	1.29×10^{-6}
$P.E$	-	33.44	78.64

4.2.4 Surface Wettability

Comparison of wettability of samples before and after treatment processes were made. Figure 4.11 shows the side view optical images of water droplet on the substrate (a), anodized with sulphuric acid (b) and heat-treated sample at $450^\circ C$ which demonstrates the wettability changes in each form. Aluminium substrate has neither hydrophobic nor hydrophilic surface, which has water contact angle of 89.2 degree. Anodizing of AA7075 in sulphuric acid shows great effect in diminishing the contact angle of which the water contact angle becomes 28.1 degree. Hydrophilic property is more obviously in heat-treated sample at $450^\circ C$ as it has relative low water contact angle of 18.3 degree. Hence, it is clearly shown that anodizing with sulphuric acids without treatment does not have any effect in enhancing the surface hydrophobicity of aluminium. Therefore, the corrosion resistance also will not be improved.

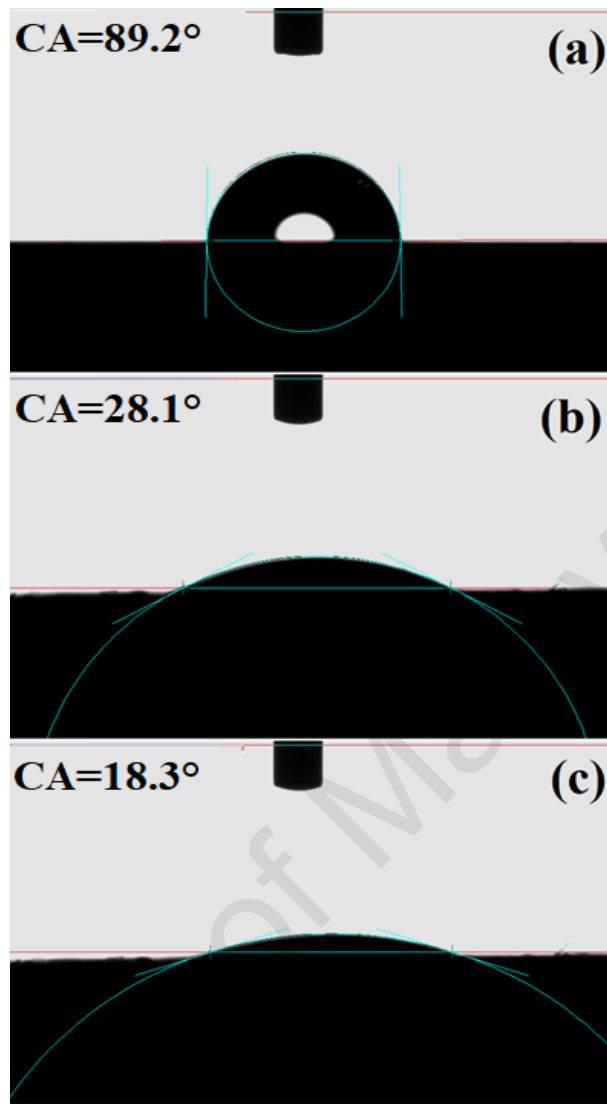


Figure 4.11: (c) heat-treated sample at 450°C.

In fact, porous oxide layer formed on the substrate surface during anodization normally consists of water in small amount and the porous layer is not in regular form. Decrease in the water contact area of anodized aluminium sample can be explained by the tri-dimensional hydrophilic property. During anodization process, hydroxide is formed due to the immersion of aluminium sample in aqueous solution which also known as electrolyte in this thesis. Hydroxide locates in the oxide film will undergo continuous growth and physical force enables free water molecular adsorbed to hydroxide. Hence, the anodized aluminium shows hydrophilic property. Majority of the aluminium with

hydrophobic surface which has high water contact angle surface that produced by organic chemical coating (Such as oxide anodic film) will lose its hydrophobicity when it has been immersed into the aqueous solution. The results obtained are consistent with previous studies (Zheng et al., 2010; Sakairi and Goyal, 2016).

Electrolyte or anodizing solution is very crucial parameter that affect surface wettability of aluminium. The finding from wettability test can deduce that further treatment shall be carried out in order to achieve hydrophobicity surface through formation of regular pores.

University of Malaysia

CHAPTER 5: Conclusion

In the current research study, aluminium oxide nano-porous is successfully formed on AA7075 surface through the anodization with sulphuric acid. Characterization study on the corrosion behavior of the synthesized aluminium oxide nano-porous layer is carried out as well as comparison before and after heat-treatment. Surface characterization studies suggest that anodizing and annealing have significant impact on the surface morphology of the aluminium oxide nano-porous.

Findings from the wettability study reveal that the heat treated AA7075 surface demonstrates hydrophilic properties. However, its wettability is improved through anodization. It is suggested to have further study on the parameter of the annealing process such as temperature and duration of treatment in order to have better corrosion resistance. Optimum processing parameters to obtain hydrophobic surface of AA7075 has to be achieved in order to reduce the wettability. With smaller surface contact angle, the potential for corrosion to take place also can be lowered. Surface hardness also studied associate with AA7075 corrosion behavior. Anodized AA7075 has better surface hardness compared to the substrate and heat treated AA7075, hence the material has better protection from the corrosion. Regular and highly ordered pore size of aluminium oxide nano-porous layer is very crucial to obtain optimum resistance of corrosion as protection layer.

Prior to heat treatment, AA7075 has corrosion rate of 4×10^{-6} and consequently the corrosion protection value is relatively low which is only 33.44%. However, the corrosion rate of AA7075 reduced to 1.29×10^{-6} and corrosion protection value has increased by 45.20%. Based on the polarization evaluation, annealing is able to improve corrosion resistance of AA7075.

Current research work is aimed in corrosion study of AA7075 with surface modifications (anodization and heat-treatment) through formation of aluminium oxide nano-porous layer formed. Observations and discussions are made on the corrosion behavior in terms of aluminium oxide nano-porous microscopy study, wettability, adhesive strength (associated with delamination of the layer) and hardness of the layer formed. The novelty of this work is to increase the accessibility of the surface modifications on improving the corrosion resistance of AA7075. The data collected can be used as reference of future corrosion research for the applications of AA7075.

Ongoing work can be focused on the following parameters:

- fabrication of oxidized aluminum layer with various thickness.
- vary the electrochemical process in terms of anodizing aluminium with different types of electrolytes which will lead to formation of pore with various diameter.
- Further investigations can be conducted on the formation of aluminium oxide nano-porous arrays with ordered and consistent diameter to increase the corrosion resistant of the AA7075.

REFERENCES

Abrahami, S., de Kok, J., Terryn, H. and Mol, J. (2017). Towards Cr(VI)-free anodization of aluminum alloys for aerospace adhesive bonding applications: A review. *Frontiers of Chemical Science and Engineering*, 11(3), pp.465-482.

AZoM.com. (2004). *Aluminium and Aluminium Alloys - Heat Treatment of Aluminium and Aluminium Alloys*. [online] Available at: <https://www.azom.com/article.aspx?ArticleID=2540> [Accessed 27 Nov. 2018].

Burns, T. (2018). / *Characteristics of Heat Treatable vs. Non Heat Treatable Aluminum Alloys*. [online] Fabricatingandmetalworking.com. Available at: <http://www.fabricatingandmetalworking.com/2014/02/characteristics-of-heat-treatable-vs-non-heat-treatable-aluminum-alloys/> [Accessed 11 Nov. 2018].

Corrosion-doctors.org. (2018). *Corrosion history*. [online] Available at: <https://corrosion-doctors.org/Corrosion-History/Introduction.htm> [Accessed 11 Nov. 2018].

Corrscience.com. (2011). Corr Science » Principles of Corrosion. [online] Available at: <http://www.corrscience.com/products/corrosion/intro-to-corrosion/principles-of-corrosion/> [Accessed 3 Dec. 2018].

Crawford, GA, Chawla, N., Das, K., Bose, S., & Bandyopadhyay, A. (2007). Microstructure and deformation behavior of biocompatible TiO₂ nanotubes on titanium substrate. *Acta Biomaterialia*, 3(3), 359-367.

Dehnavi, V., Luan, B. L., Liu, X. Y., Shoosmith, D. W., & Rohani, S. (2015). Correlation between plasma electrolytic oxidation treatment stages and coating microstructure on aluminum under unipolar pulsed DC mode. *Surface and Coatings Technology*, 269, 91-99.

Diggle, J., Downie, T. and Goulding, C. (1969). Anodic oxide films on aluminum. *Chemical Reviews*, 69(3), pp.365-405.

Elham Farouk, M. (2018). *Removal of Organic Compounds from Water by Adsorption and Photocatalytic Oxidation*. [online] Ethesis.inp-toulouse.fr. Available at: <http://ethesis.inp-toulouse.fr/archive/00001569/01/mohamed.pdf> [Accessed 10 Nov. 2018].

Fallahi, A., Hosseini-Toudeshky, H., & Ghalehbandi, S. M. (2014). Effect of heat treatment on mechanical properties of ECAPed 7075 aluminum alloy. In *Advanced Materials Research* (Vol. 829, pp. 62-66). Trans Tech Publications.

Fan, L., Lu, H., & Leng, J. (2015). Performance of fine structured aluminum anodes in neutral and alkaline electrolytes for Al-air batteries. *Electrochimica Acta*, 165, 22-28.

Foley, R. T. (1986). Localized corrosion of aluminum alloys—a review. *Corrosion*, 42(5), 277-288.

Glanvill, S. J. M. (2018). *Atmospheric corrosion of AA2024 in ocean water environments* (Doctoral dissertation, University of Birmingham).

Hanke, S., Schymura, M., Stickel, D. and Fischer, A. (2013). Wear Behaviour of Nanoporous Alumina Coatings from Anodic Oxidation. In: *World Tribology Congress 2013*.

Hannard, F., Pardoën, T., Maire, E., Le Bourlot, C., Mokso, R., & Simar, A. (2016). Characterization and micromechanical modelling of microstructural heterogeneity effects on ductile fracture of 6xxx aluminium alloys. *Acta Materialia*, 103, 558-572.

Hatch, J. (1984). *Aluminium*. Metals Park, OH: ASM, pp.1-20.

Hinds, G. ed., (n.d.). *The Electrochemistry of Corrosion*. pp.1-12.

Kairy, S. K., Rometsch, P. A., Diao, K., Nie, J. F., Davies, C. H. J., & Birbilis, N. (2016). Exploring the electrochemistry of 6xxx series aluminium alloys as a function of Si to Mg ratio, Cu content, ageing conditions and microstructure. *Electrochimica Acta*, 190, 92-103.

Kashima-coat.com. (2018). *About Anodizing - About Anodizing & Aluminum | Next-generation anodize boasting light weight, high lubrication, and superb wear resistance. The answer is Miyaki's Kashima Coat.* [online] Available at: <http://www.kashima-coat.com/global/aluminum/anodized-aluminum.html> [Accessed 19 Nov. 2018].

Krishna, L. R., Poshal, G., Jyothirmayi, A., & Sundararajan, G. (2015). Relative hardness and corrosion behavior of micro arc oxidation coatings deposited on binary and ternary magnesium alloys. *Materials & Design*, 77, 6-14.

Li, X. P., Wang, X. J., Saunders, M., Suvorova, A., Zhang, L. C., Liu, Y. J., ... & Sercombe, T. B. (2015). A selective laser melting and solution heat treatment refined Al–12Si alloy with a controllable ultrafine eutectic microstructure and 25% tensile ductility. *Acta Materialia*, 95, 74-82.

Liu, Y., Mol, J. and Janssen, G. (2016). Combined Corrosion and Wear of Aluminium Alloy 7075-T6. *Journal of Bio- and Tribo-Corrosion*, 2(2).

McCafferty, E. (2010). *Introduction to corrosion science*. New York: Springer.

Melendres, C., Van Gils, S. and Terryn, H. (2001). Toward a quantitative description of the anodic oxide films on aluminum. *Electrochemistry Communications*, 3(12), pp.737-741.

Miller, W. S., Zhuang, L., Bottema, J., Wittebrood, A., De Smet, P., Haszler, A., & Vieregge, A. (2000). Recent development in aluminium alloys for the automotive industry. *Materials Science and Engineering: A*, 280(1), 37-49.

Niensch, K., Choi, J., Schwirn, K., Wehrspohn, R. and Gösele, U. (2002). Self-ordering Regimes of Porous Alumina: The 10 Porosity Rule. *Nano Letters*, 2(7), pp.677-680.

Niensch, K., Müller, F., Li, A. P., & Gösele, U. (2000). Uniform nickel deposition into ordered alumina pores by pulsed electrodeposition. *Advanced Materials*, 12(8), 582-586.

Parkhutik, V., Belov, V. and Chernykh, M. (1990). Study of aluminium anodization in sulphuric and chromic acid solutions—II. Oxide morphology and structure. *Electrochimica Acta*, 35(6), pp.961-966.

Poinern, G., Ali, N. and Fawcett, D. (2011). Progress in Nano-Engineered Anodic Aluminum Oxide Membrane Development. *Materials*, 4(3), pp.487-526.

Poinern, G., Ali, N. and Fawcett, D. (2011). Progress in Nano-Engineered Anodic Aluminum Oxide Membrane Development. *Materials*, 4(3), pp.487-526.

Ponthiaux, P., Wenger, F. and Celis, J. (n.d.). *Tribocorrosion: Material Behavior Under Combined Conditions of Corrosion and Mechanical Loading*. [online] p.82. Available at: <http://www.intechopen.com> [Accessed 18 Nov. 2018].

Prasad, S. and Quijano, J. (2006). Development of nanostructured biomedical micro-drug testing device based on in situ cellular activity monitoring. *Biosensors and Bioelectronics*, 21(7), pp.1219-1229.

Sakairi, M. and Goyal, V. (2016). Improvement of Corrosion Resistance of Aluminium Alloy with Wettability Controlled Porous Oxide Film. *Corrosion Science and Technology*, 15(4), pp.166-170.

Santa Coloma, P., Izagirre, U., Belaustegi, Y., Jorcin, J. B., Cano, F. J., & Lapeña, N. (2015). Chromium-free conversion coatings based on inorganic salts (Zr/Ti/Mn/Mo) for aluminum alloys used in aircraft applications. *Applied Surface Science*, 345, 24-35.

Sarraf, M. (2018). *MECHANICAL AND BIOLOGICAL BEHAVIORS OF TITANIA AND TANTALA NANOTUBULAR ARRAYS DECORATED WITH SILVER OXIDE ON Ti-6Al-4V ALLOY* MASOUD SARRAF FACULTY OF ENGINEERING UNIVERSITY OF MALAYA KUALA LUMPUR 2017. Ph.D. University of Malaya Kuala Lumpur.

Schuman, T. P. (2018). Protective coatings for aluminum alloys. In *Handbook of Environmental Degradation of Materials (Third Edition)* (pp. 423-448).

Sharma, M., Eden, T. and Golesich, B. (2014). Effect of Surface Preparation on the Microstructure, Adhesion, and Tensile Properties of Cold-Sprayed Aluminum Coatings on AA2024 Substrates. *Journal of Thermal Spray Technology*, 24(3), pp.410-422.

Sheasby, P. and Pinner, R. (2001). The Surface Treatment and Finishing of Aluminium and Its Alloys. 1(6).

Shih, T., Lee, T. and Jhou, Y. (2014). The Effects of Anodization Treatment on the Microstructure and Fatigue Behavior of 7075-T73 Aluminum Alloy. *MATERIALS TRANSACTIONS*, 55(8), pp.1280-1285.

Speller, F.N. (1951), *Corrosion Causes and Prevention*, McGraw- Hill Book Co., Inc, New York and London, p.8.

Talbot, D. E., & Talbot, J. D. (2018). *Corrosion science and technology*. CRC press.

Tavares, A. M. G., Ramos, W. S., de Blas, J. C. G., Lopes, E. S. N., Caram, R., Batista, W. W., & Souza, S. A. (2015). Influence of Si addition on the microstructure and mechanical properties of Ti–35Nb alloy for applications in orthopedic implants. *Journal of the mechanical behavior of biomedical materials*, 51, 74-87.

Tilley, R. J. (2010). *Colour and the optical properties of materials: An exploration of the relationship between light, the optical properties of materials and colour*. Hoboken, NJ: Wiley. Available at: <http://pilkington.com/products/bp/bybenefit/specialapplications/tecglass/> [Accessed 4 Nov. 2018].

Villegas, J. (2017). *Aluminium Highlights*.

Wang, H., Sun, W. and Xing, Y. (2013). *Microstructure Analysis on 6061 Aluminum Alloy after Casting and Diffuses Annealing Process*. *Physics Procedia*, 50, pp.68-75.

Zhao, Y., Chen, M., Zhang, Y., Xu, T. and Liu, W. (2005). A facile approach to formation of through-hole porous anodic aluminum oxide film. *Materials Letters*, 59(1), pp.40-43.

Zhecheva, A., Sha, W., Malinov, S., & Long, A. (2005). Enhancing the microstructure and properties of titanium alloys through nitriding and other surface engineering methods. *Surface and Coatings technology*, 200(7), 2192-2207.

Zheng, M., Jha, H., Sakairi, M. and Kikuchi, T. (2010). Influence of Wettability on Corrosion Resistance of Anodized Aluminum in NaCl Solution. *Zairyo-to-Kankyo*, 59(9), pp.335-337.